Permo-Triassic extension and related HT/LP metamorphism in the Austroalpine - Southalpine realm

by

Ralf SCHUSTER, Susanna SCHARBERT, Rainer ABART & Wolfgang FRANK

with 12 Figures and 5 Tables

Key words:
Austroalpine
Permo-Triassic extension
HT/LP metamorphism
Geodynamics
Geochronology

Schlüsselwörter:
Ostalpin
Permotriassische Extension
HT/LP Metamorphose
Geodynamik
Geochronologie

Addresses of the authors:
RALF SCHUSTER and WOLFGANG FRANK
Institut für Geologie
Universität Wien
Althanstraße 14
A-1090 Vienna, Austria
E-mail: Ralf.Schuster@univie.ac.at
Wolfgang.Frank@univie.ac.at

SUSANNA SCHARBERT
Geologische Bundesanstalt
Rasumofskygasse 23
A-1030 Vienna, Austria
E-mail: sscharbert@cc.geolba.ac.at

RAINER ABART
Mineralogisch Petrographisches Institut
Universitaet Basel
Bernoulllistrasse 30
CH-4056 Basel
E-mail: rainer.abart@unibas.ch

Mitt. Ges. Geol. Bergbaustud. Österr.	45	S.111-141	Wien 2001

Contents

Kurzfassung....112
Abstract....112
1. Introduction....113
2. Geological settings....113
3. Analytical techniques....115
4. Permo-Triassic basement lithologies: petrography and age data....115
4.1. Austroalpine Units south of the SAM....115
4.2. Austroalpine Units north of the SAM and west of the Gurktal Nappe System....122
4.3. Austroalpine Units north of the SAM and east of the Gurktal Nappe System....124
5. Discussion....128
5.1. Typical features....129
5.1.1. Relations of magmatic and metamorphic rocks....129
5.1.2. Peak metamorphism and cooling history....129
5.1.3. Metamorphic conditions....130
5.2. Extension of the Permo-Triassic metamorphic event....133
5.2.1. Southalpine....133
5.2.2. Extension of the event to the east and north....133
5.3. Thermal evolution and geotectonic setting....134
5.3.1. P-T-t evolution....134
5.3.2. Geotectonic setting....135
5.3.3. Sedimentary cover....135
5.4. Plate tectonic environment and paleogeographic framework....135
Acknowledgements....137
References....137

Kurzfassung

In permotriassischer Zeit wurde das Ostalpin von weitverbreitetem Magmatismus, einer Hochtemperatur/Niederdruck (HT/LP) Metamorphose und von extensioneller Tektonik erfaßt. Die Auswirkungen dieses Ereignisses lassen sich gut im Drauzug-Goldeck-Kreuzeck- und im Silvrettagebiet studieren, wo weitgehend komplete Profile durch die permotriassische Kruste, von den Sedimenten bis in die mittlere Kruste erhalten sind. Die Metamorphose ist durch einen hohen geothermischen Gradienten von etwa 45 °C/km charakterisiert und erreicht amphibolit- bis granulitfazielle Bedingungen. Sie ist zeitgleich mit der Platznahme von Gabbros, Graniten, Pegmatiten sowie verschiedenen vulkanischen Gesteinen. Die Magmatite sind häufig, gegenüber den Umgebungsgesteinen, volumensmäßig jedoch unbedeutend. Der Metamorphosehöhepunkt wurde um 270 Ma erreicht, die Gesteine wurden danach nicht exhumiert sondern verweilten in der Kruste, wo sie bis etwa 190 Ma langsam abkühlten.
Für das Südalpin ist eine sehr ähnliche permotriassische Entwicklung belegt. Intrusionen gabbroider Schmelzen in der Ivrea Zone werden in der Literatur als magmatic underplating an der Krusten/Mantel Grenze interpretiert. Gegen Osten läßt sich das permotriassische Ereignis bis in die Karpaten und ins südöstliche Ungarn verfolgen.
Das permotriassische Ereignis wird mit Extension der Lithosphäre in Zusammenhang gebracht. Im unteren Perm entstanden im lithospherischen Mantel Druckentlastungsschmelzen, die nahe der Krusten/Mantel Grenze intrudierten. In der Kruste kam es zu einer HT/LP Metamorphose und zu anatektischer Schmelzbildung. Ab dem oberen Perm kühlte die Lithosphäre ab und anhaltende Subsidenz führte zur Ablagerung mächtiger permomesozoischer Sedimentfolgen. Im Anis kam es durch Rifting zur Öffnung des Meliata Ozeans.

Abstract

During Permo-Triassic times the Austroalpine units were affected by widespread magmatism, high temperature/low pressure metamorphism (HT/LP) and extensional tectonic. Features of this event can be studied in the Drauzug-Goldeck-Kreuzeck and Silvretta areas where more or less complete sections through the Permo-Triassic crust, from the sedimentary successions down to the middle crust have been preserved. Metamorphism was characterised by a geothermal field gradient of more than 45°C/km, and reached amphibolite to granulite facies conditions. It was accompanied by intrusions of gabbros, granites and pegmatites and extensive volcanism. The igneous rocks are common but volumetrically subordinate with respect to the country rocks. Peak metamorphism was reached at about 270 Ma, subsequently the rocks were not exhumed but cooled down until c. 190 Ma, when the steady state geotherm was reached again.
In the Southalpine realm a similar evolution is visible. In the literature basic intrusions of the Ivrea Zone are interpreted as magmatic underplating near the crustal/mantle boundary. To the east the Permo-Triassic event can be traced to the Carpathians and to southeast Hungary.
The Permo-Triassic extensional event is related to extension of the lithosphere. In early Permian times decompression melts from the lithospheric mantle intruded near to the

crustal/mantle boundary. They caused a HT/LP metamorphism and anatectic melting in the crust. Since the late Permian cooling of the lithosphere was responsible for ongoing subsidence and the deposition of thick sedimentary piles. Anisian rifting caused opening of the Meliata ocean.

1. Introduction

Within the Alpine orogenic belt metamorphic rocks occur in a complex nappe pile (Fig. 1). They show variable metamorphic grades and exhibit prograde or polyphase metamorphic evolutions. As regional metamorphism is the result of continent-continent collision and as the area was affected by the Variscan and the Alpine collisional event, it is generally accepted that the rocks got their major thermal imprints during Variscan (390 – 300 Ma) and/or Alpine (120 – 20 Ma) times (e.g. DESMONS et al. 1999a, HOINKES et al. 1999, NEUBAUER et al. 1999b). However, evidence for an additional Permo-Triassic metamorphic event, characterised by high-temperature/low pressure (HT/LP) conditions has been documented in the Southalpine (e.g. BRODIE et al. 1989, LARDEAUX & SPALLA 1991, DIELLA et al. 1992, SANDERS et al. 1996) and nowadays also in the Austroalpine domain (SCHUSTER & THÖNI 1996, LICHEM et al. 1997, HABLER & THÖNI 1998).

This paper focuses on the Permo-Triassic thermal and metamorphic history of the Austroalpine realm. It is based on lithological studies and geochronological data from Austroalpine units and gives an overview on data from the Southalpine domain. The results are discussed in the frame of the geodynamic history of the area, which is generally known from the sedimentary record and can be summarised as follows: Graben structures and sedimentation of post-Variscan molasse sediments indicate thinning of the thickened Variscan crust by orogenic collapse and erosion during Upper Carboniferous to Lower Permian time (WOPFNER 1984, ZIEGLER 1993, BONIN et al. 1993). In the Middle Permian marine transgressions accompanied by fine-grained clastic, evaporitic and carbonatic sedimentation can be observed (e.g. STAMPFLI & MOSAR 1999). The sediments argue for a relatively flat topography, a low altitude and a normal thickness of the lithosphere because of isostatic reasons. Permian extension in the northern part of the Adriatic microplate and in the southern part of Europe is documented by extensional structures, a locally observed HT/LP metamorphism and intense magmatic activity.

For the Southalpine realm BERTOTTI et al. (1993) described large scale extensional structures. Based on the sedimentary record, extension started with the highest rates before 250 Ma and continued, maybe discontinuously until middle Jurassic time. Permo-Triassic magmatic rocks include volcanic rocks (BARTH et al. 1994, SCHALTEGGER & BRACK 1999), gabbros (SILLS 1984, BÜRGI & KLÖTZLI 1987, PIN 1986, QUICK et al. 1992), granites (BORSI et al. 1972, FERRARA & INNOCENTI 1974) and pegmatites (SANDERS et al. 1996). Evidence for a Permian HT/LP metamorphic event has been documented for the Ivrea Zone (SCHMIDT & WOOD 1976, BRODIE et al. 1989, COLOMBO & TUNESI 1999) and the Dervio-Oligasca basement (DIELLA et al. 1992, SILETTO et al. 1993, SANDERS et al. 1996, DI PAOLA & SPALLA 2000).

In the Austroalpine realm, the post-Variscan/pre-Alpine evolution is highly obscured by the intense Alpine overprint. Nevertheless evidences for a Permo-Triassic extensional event and crustal thinning exist: The huge piles of Permo-Triassic sediments indicate subsidence of their basement. As in the Southalpine quartzporphyric volcanic rocks are common as layers and pebbles within the Permian transgressive series, whereas basic tuffs occur in the Triassic sedimentary successions (e.g. GAAL 1966, TOLLMANN 1977, 1985). Geochronological age data yielded Permian and Triassic ages on granites (MORAUF 1980), gabbroic rocks (MILLER & THÖNI 1997, PUMHÖSL et al. 1999) and numerous pegmatites (e.g. BORSI et al. 1980, THÖNI & MILLER 2001). However a Permian metamorphic event is documented only for a few localities (SCHUSTER & THÖNI 1996, LICHEM et al. 1997, HABLER & THÖNI 1998), whereas a HT/LP imprint of proposed Variscan or uncertain age has been recognised in many places (e.g. WEISSENBACH 1975, FRANK et al. 1983, HOKE 1990, DRAGANITS 1998).

In this study Austroalpine HT/LP assemblages and magmatic rocks were investigated to get information on their genetic relations and on the extension and intensity of the Permo-Triassic thermal event.

2. Geological settings

The Alpine mountain belt is a complex nappe stack (Fig. 1) built by the following plate tectonic units (e.g. TOLLMANN 1977): The former southern margin of Europe is represented by the Helvetic Zone and the Central Gneisses of the Tauern Window, which are in comparable tectonic position (FROITZHEIM et al. 1986). Above remnants of the Jurassic Penninic ocean are present, which was located in a southern position, prior to its closure during the Alpine collisional event in Tertiary times. The Austroalpine and the Southalpine are the uppermost tectonic elements. They are parts of the Adriatic microplate, which represented the upper plate during the closure of the Penninic ocean. They are separated by the Periadriatic Lineament (PAL) but show many similarities with respect to their pre-Alpine metamorphic basement, their Palaeozoic sequences and their Mesozoic cover series. However the Austroalpine is much more tectonised because it acted as the tectonic lower plate during the Eo-Alpine (Cretaceous) closure of the Triassic Meliata-Hallstatt ocean. Tectonic slices of this oceanic realm only occur in the easternmost part of the Austroalpine in a few outcrops (MANDL & ONDREJICKOVA 1993).

The Austroalpine crystalline units form an east-west trending belt located between the Austroalpine Northern Calcareous Alps to the north and the PAL respectively the Southalpine to the south (Fig. 1). The pre-Alpine tectonic arrangement and metamorphic zonation of the area is obliterated to a variable grade because of the Alpine overprints. The Eo-Alpine metamorphic imprint reaches up to eclogite facies and subsequent amphibolite facies conditions in some areas. The line connecting the southernmost occurrences of the Eo-Alpine eclogites was defined by HOINKES et al. (1999) as the “southern border of Alpine metamorphism” (SAM).

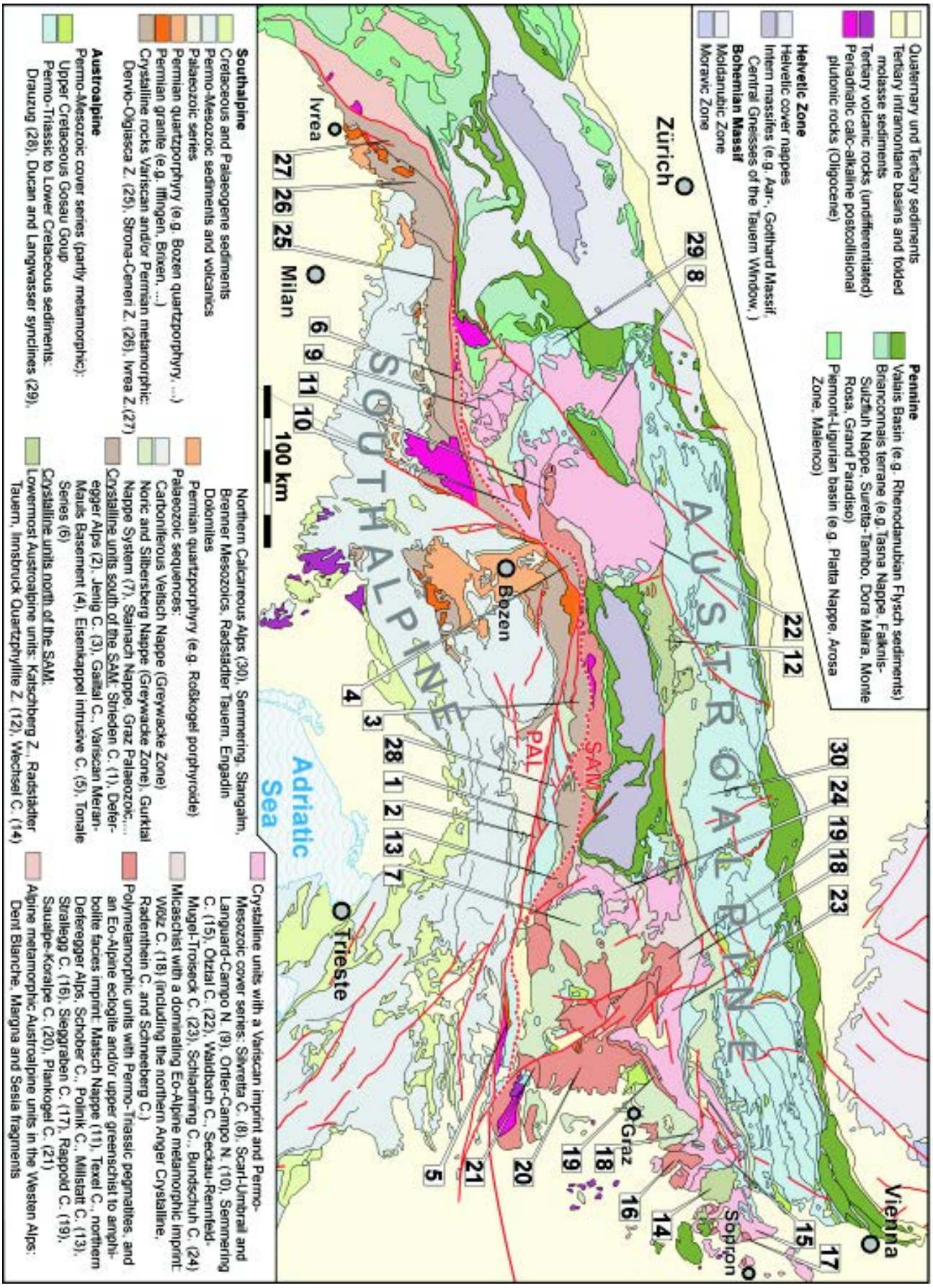

Fig. 1: Tectonic map of the Alps. The numbers refer to units discussed in the text. PAL… Periadriatic Lineament, SAM… Southern limit of Alpine Metamorphism (HOINKES et al. 1999).

Within the units north of the SAM the Eo-Alpine metamorphic conditions are generally decreasing from eclogite and/or amphibolite facies just at the SAM to low-grade or very low-grade conditions in the north (HOINKES et al. 1999). In the eastern part of the belt this zonation is due to a tectonic inversion of the metamorphic grades by polyphase west to north-directed thrust tectonics (FRANK et al. 1983, RATSCHBACHER 1986, GENSER & NEUBAUER 1989, SCHUSTER et al. 2001). South of the SAM the pre-Alpine lithologies are well preserved because Alpine thermal overprints reach lowermost greenschist facies for maximum and tectonics are restricted to folding and block faulting. Permian magmatic rocks, as well as andalusite and sillimanite-bearing HT/LP assemblages occur on both sides of the SAM. To the north the alumosilicate phases are partly or fully transformed into kyanite.

3. Analytical techniques

Garnets with optical and chemical distinct cores that have been used for dating were selected by mineral chemical data and back-scattered-electron images. They were cut in slices of about 0.5 mm thickness and mounted on slides. Subsequently the rims were removed by a saw and the remaining slices of the cores were crushed in a mortar.

Minerals used for isotope determinations were hand-picked under a binocular microscope, except muscovite and biotite which were separated on a vibrating table and by grinding in alcohol. To remove surface contaminations mineral concentrates used for Sm-Nd and Rb-Sr analyses were leached in 2.5 N HCl before decomposition for 5 minutes at about 50 °C. Chemical sample digestion and element separation follows the procedure outlined by THÖNI & JAGOUTZ (1992). Overall blank contributions are ≤ 0.2 ng for Nd and Sm, and ≤ 2 ng for Rb and Sr. Nd and Sm concentrations were determined by isotope dilution, using a mixed ^{147}Sm-^{150}Nd spike, and run as metals on a Finnigan®MAT 262 multicollector mass spectrometer. Nd was ionised using a Re double filament. Within-run isotope fractionation was corrected for $^{146}Nd/^{144}Nd = 0.7219$. All errors quoted in Tables 2 and 3 correspond to 2σ of the block mean (1 block = 10 isotope ratios). The $^{143}Nd/^{144}Nd$ ratio for the La Jolla international standard during the course of this investigation was 0.511846 ± 8 (35 runs). Errors for the $^{147}Sm/^{144}Nd$ ratio are ±1%, or smaller, based on iterative sample analysis and spike recalibration. For the calculation of depleted mantle (DM) ages the following model parameters were used: $^{147}Sm/^{144}Nd = 0.222$, $^{143}Nd/^{144}Nd = 0.513114$ (MICHARD et al. 1985). A linear evolution of the Nd isotope composition of the DM is assumed throughout geological time, εNd values are calculated relative to CHUR. Sr and Rb concentrations were determined using a VG® Micromass M 30 and Ta filaments. Through the course of this study the value for the NBS 987 Sr standard was 0.71011 ± 1. Maximum errors for $^{87}Rb/^{86}Sr$ ratios are estimated to be ± 1%.

For Ar-Ar age determinations the mineral concentrates were irradiated at the 9MW ASTRA reactor at the Austrian Research Center Seibersdorf and analysed using standard procedures with a VG-5400 Fisons Isotopes® mass spectrometer. Age calculation was done after corrections for mass discrimination and radioactive decay using the formulas given in DALRYMPLE et al. (1984). J-values are determined with internal laboratory standards, calibrated by international standards including muscovite Bern 4M (BURGHELE 1987) and amphibole MMhb-1 (SAMSON & ALEXANDER 1987). The errors given on the calculated age of an individual step include only the 1σ error of the analytical data. The error of the plateau and total gas ages includes an additional error of ± 0.4 % on the J-value, based on standard reproducibility.

Mineral composition data were obtained with an ARL SEMQ microprobe by energy and/or wavelength-dispersive spectrometry at the universities of Vienna and Innsbruck. Accelerating voltage was 15 kV and sample current 20 nA. Natural and synthetic standards were used for calibration.

Geochronological ages represent formation or cooling ages of rocks and minerals (JÄGER 1979). In this paper U-Pb ages of zircons and monazites as well as Sm-Nd isochrone ages are interpreted as crystallisation ages of magmatic rocks or formation ages of metamorphic minerals respectively. Rb-Sr whole-rock errorchrones reflect isotopic homogenisation of large rock volumes, whereas muscovite-whole rock isochrones are cooling ages below 500 °C. K-Ar and Ar-Ar muscovite ages are cooling ages below 400 °C in lithologies which cool down from higher metamorphic temperatures and represent formation ages in rocks which experienced a metamorphic imprint of temperatures below. K-Ar, Ar-Ar and Rb-Sr ages are cooling ages below 300 °C.

4. Permo-Triassic basement lithologies: petrography and age data

This chapter summarises P-T estimations and radiometric age data of Permo-Triassic metamorphic and magmatic rocks from Austroalpine units. Numbers beside the names of the units correspond to Fig. 1 and Table 5. GPS-coordinates of the samples are given in Table 1. All age and isotope data are listed in Tables 2, 3 and 4 the P-T data from the literature are summarised in Table 5.

4.1. Austroalpine units south of the SAM

At first well preserved pre-Alpine metamorphic succession south of the SAM are described. They represent segments of the Permo-Mesozoic crust with weak Alpine overprints.

A more or less continuous section through a Permo-Triassic middle and upper crust, up into the Permian sedimentary cover, has been preserved in the Kreuzeck-Goldeck-Drauzug area (SCHUSTER & FAUPL 2001). The Mesozoic sediments of the Drau Range (28) transgressed on top of the Goldeck and Gaugen Complexes which form the upper crust, the Strieden Complex (1) below represents the middle crust. The latter shows a zonation expressed in mineral assemblages, the occurrence of pegmatites and typical cooling ages for different structural levels. The deepest struc-

sample	lithology	unit	locality	ÖK50	N	E
RS13/97	And-Bt schist	Strieden Complex	Steinwander Hochalm, Kreuzeckg., Carinthia	181	46°52'46"	013°03'25"
RS14/97	St-Grt micaschist	Strieden Complex	Steinwander Hochalm, Kreuzeckg., Carinthia	181	46°52'46"	013°03'25"
RS23/99	Sil-Bt schist	Strieden Complex	E' Latischhütte, Ragga, Kreuzeckg., Carinthia	181	46°53'00"	013°07'00"
RS27/99	St-Sil schist	Strieden Complex	N' Strieden, Kreuzeckgruppe, Carinthia	181	46°52'49"	013°06'35"
RS25/99	St-And schist	Strieden Complex	N' Strieden, Kreuzeckgruppe, Carinthia	181	46°52'49"	013°06'35"
RS43/99	Grt pegmatite	Strieden Complex	S' Schneestellkopf, Kreuzeckgruppe, Carinthia	181	46°52'43"	013°08'40"
RS52/99	Grt-Ms schist	Strieden Complex	E' Kleines Hochkreuz, Carinthia	181	46°49'53"	013°06'15"
RS55/99	Grt-Ms schist	Strieden Complex	In der Kirschen, Kreuzeckgruppe, Carinthia	181	46°49'12"	013°06'17"
RS4/00	Grt-St micaschist	Strieden Complex	S' Striedenkopf, Kreuzeckgruppe, Carinthia	181	46°52'00"	013°06'44"
RS35/00	Grt pegmatite	Strieden Complex	S' Salzkofel, Kreuzeckgruppe, Carinthia	181	46°49'46"	013°15'42"
RS69/00	And-Qtz-Ms vein	Strieden Complex	S' Schneestellkopf, Kreuzeckgruppe, Carinthia	181	46°52'	013°08'
RS7/00	micaschist	Gaugen Complex	S' Putzen, Kreuzeckgruppe, Carinthia	181	46°28'25"	013°12'02"
RS11/00	Sil-Bt schist	S' block Deferegger A.	Tönig, Deferegger Alpen, Osttirol	178	46°54'52"	012°23'43"
RS13/00	Sil-Bt schist	S' block Deferegger A.	Michelbachtal, Deferegger Alpen, Osttirol	178	46°52'24"	012°35'16"
RS14/00	Sil-Bt schist	S' block Deferegger A.	Michelbachtal, Deferegger Alpen, Osttirol	178	46°53'03"	012°35'11"
RS9/98	And-Bt schist	Jenig Complex	N' Jenig, Gailtal, Carinthia	198	46°37'55"	013°15'15"
RS11/98	And-Bt schist	Jenig Complex	N' Jenig, Gailtal, Carinthia	198	46°37'55"	013°15'15"
RS13/98	And-Bt schist	Jenig Complex	N' Jenig, Gailtal, Carinthia	198	46°37'55"	013°15'15"
RS22/96	Grt pegmatite	Millstatt Complex	Millstätter Alpe, Radenthein, Carinthia	183	46°48'02"	013°40'47"
31-35/83	pegmatite	Millstatt Complex	Lieserschlucht, Millstätter Seenr., Carinthia	182	46°48'	013°30'
36-40/83	pegmatite	Millstatt Complex	Wolfsberg, Millstätter Seenrücken, Carinthia	182	46°48'	013°31'
41-48/83	pegmatite	Millstatt Complex	Laas, Millstätter Seenrücken, Carinthia	200	46°43'	013°40'
RS7/96	And-Bt schist	Strallegg Complex	ESE' Kaltes Bründl, Ritzing, Burgenland	107	47°38'35"	016°31'31"
RS8/96	granatite	Strallegg Complex	ESE' Kaltes Bründl, Ritzing, Burgenland	107	47°38'35"	016°31'31"
RS3/97	Ky-Grt micaschist	Strallegg Complex	Walleiten, Hartberg, Styria	136	47°17'18"	015°57'10"
RS9/97	Ky-bearing gneiss	Strallegg Complex	ESE' Fünfhöf bei Greith, N' Hartberg, Styria	136	47°18'21"	015°56'33"
RS10/97	Ky-bearing gneiss	Strallegg Complex	ESE' Fünfhöf bei Greith, N' Hartberg, Styria	136	47°18'21"	015°56'33"
Ab9	pegmatite	Strallegg Complex	quarry Stubenberg, Styria	166	47°14'41"	015°47'15"
Ab10	granite	Strallegg Complex	quarry Krughofkogel, Rabenwald, Styria	135	47°17'11"	015°45'19"
RS44/97	Grt micaschist	Wölz Complex	500m south of Glattjoch, alt. 1850m, Styria	129	47°19'12"	014°13'11"
RS1/95	Grt pegmatite	Rappold Complex	Pfingstnergraben, Bretstein v. d. Kirche, Styria	130	47°19'12"	014°25'39"
RS8/95	Grt-St micaschist	Rappold Complex	Eicher, Vorderschönberg, Unzmarkt, Styria	160	47°10'25"	014°21'37"
RS10/95	pegmatite	Rappold Complex	Fresen, Krakaudorf, Styria	158	47°09'48"	014°01'10"
RS15/96	pegmatite	Rappold Complex	Nassel, Thomasberg, Unzmarkt, Styria	160	47°12'19"	014°25'22"
RS16/96	Grt pegmatite	Rappold Complex	Preisner, Hirschfeld, Unzmarkt, Styria	160	47°10'00"	014°26'13"
RS51/97	Grt-St micaschist	Rappold Complex	Turneralm, Steinplan, Knittelfeld, Styria	162	47°09'07"	014°56'45"
RS64/99	Grt pegmatite	Rappold Complex	Preisner, Hirschfeld, Unzmarkt, Styria	160	47°12'23"	014°25'28"
Wölz 1-5	pegmatite	Rappold Complex	Niedere Tauern, Styria			
G63	Grt micaschist	Saualpe-Koralpe C.	600m S' Noreia, Mühlen, Styria	160	47°00'40"	014°31'36"

Table 1: GPS-coordinates and localities of the samples.

tural levels and rocks of highest metamorphic grade are exposed in the north, immediately south of the SAM (represented by the Ragga-Teuchl fault zone, HOKE 1990). The whole sequence is tentatively divided in a lower and upper sillimanite-zone, andalusite-zone, staurolite-zone and garnet-zone (Fig. 2).

The uppermost garnet-zone consists of garnet-chlorite-muscovite schists and subordinate amphibolites, which exhibit a polyphase deformation (D_m, D_n) (HOKE 1990, SCHUSTER & SCHUSTER 2001). The metapelites are characterised by syndeformational assemblages of Grt + Chl + Ms/Pg + Pl + Qtz + Ilm ± Bt (Fig. 3A). Going north, and downward in the section, gneisses intercalated by layers of garnet-staurolite two-mica schists with a mineral assemblage of Grt + St ± Ky + Bt + Ms + Pl + Qtz + Ilm occur in the staurolite-zone (Fig. 3B). In the andalusite-zone below, up to several centimetres large andalusite porphyroblasts and andalusite-quartz veins occur. They are restricted to the staurolite and garnet-rich micaschist layes which represent Al-rich (24.9-26.9 wt%) metapelites with a low XMg (0.19). Andalusite as well as large biotite flakes are overgrowing the pre-existing microfabrics and the garnet porphyroblasts. Staurolite is resorbed and forms dismembered inclusions with identical optical orientation, indicating andalusite formation during prograde breakdown of staurolite by the reaction St + Ms + Qtz = And + Bt + H_2O (Fig. 3C). Another possible aluminumsilicate forming reaction is Pg + Qtz = Ab + And/Sil + H_2O (Fig. 3D). In the lowermost part of the andalusite-zone pegmatites and fibrolitic sillimanite appears. The upper sillimanite-zone is characterised by sillimanite, the continuous disappearance of staurolite with depth and the occurrence of pegmatites (HOKE 1990) (Fig. 3E). An overprinting ductile deformation (D_o), becomes more prominent with structural depth. Staurolite and garnet act as porphyroclasts whereas sillimanite growth is syndeformational. In the lower sillimanite-zone garnet disappears, the amount of muscovite is decreasing and concordant pegmatites are frequent. In the metapelites sillimanite is intergrown with biotite

sample	mineral	Sm	Nd	$^{147}Sm/^{144}Nd$	$^{143}Nd/^{144}Nd$	$2\sigma m$	$\varepsilon 0$	T^{Nd}_{DM}	Rb	Sr	$^{87}Rb/^{86}Sr$	$^{87}Sr/^{86}Sr$	$2\sigma m$
		[ppm]	[ppm]				(Nd)		[ppm]	[ppm]			
RS1/95	whole rock	3.613	10.16	0.2150	0,5122488	± 10	-7,6	1.8E+9					
	garnet	4.787	0.637	4.5521	0,5196983	± 25							
	tourmaline	0.151	0.458	0.1991	0.512134	± 25							
RS8/95	whole rock	49.85	8.986	0.1090	0.512098	± 5	-10	1.4E+9					
	garnet	0.519	1.416	1.6502	0.514982	± 7							
RS 10/95	whole rock								41.82	373.5	0.324	0.71372	± 5
RS 10/95	muscovite								332.1	54.73	17.67	0.77306	± 10
RS 15/96	whole rock								179.0	43.64	11.93	0.75713	± 12
RS 15/96	muscovite								651.4	14.85	131.9	1.10753	± 13
RS 16/96	whole rock								356.3	32.75	31.94	0.85606	± 9
RS 16/96	muscovite								2454	4.386	3404	11.985	± 3
RS 22/96	whole rock								143.0	10.46	40.30	0.89867	± 20
RS 22/96	muscovite								932.9	1.775	3986	17.287	± 5
RS3/97	garnet+inclusions	5.744	27.20	0.1277	0.511922	± 5							
	garnet	1.840	4.301	0.2585	0.512159	± 5							
RS13/97	whole rock	79.61	12.98	0.0986	0.511859	± 6	-15	1.2E+9	98.21	157.7	1.808	0.73437	± 6
	muscovite								200.9	282.3	2.064	0.73109	± 5
	biotite	1.199	0.252	0.1269	0.511952	± 10			462.5	4.917	298.0	1.67837	± 31
RS14/97	whole rock	13.377	77.29	0.1046	0.511851	± 5	-15	1.6E+9	80.70	171.5	1.366	0.74284	± 8
	muscovite								190.5	288.4	1.917	0.73635	± 8
	biotite								737.9	3.467	714.4	2.34298	± 70
	garnet	4.364	5.882	0.4486	0.512622	± 6							
	staurolite	6.380	1.098	0.1040	0.511868	± 4							
RS11/98	whole rock								372.0	248.9	4.336	0.73172	± 5
	biotite								497.6	11.80	126.7	1.08974	± 16
RS13/98	whole rock								155.4	248.6	1.813	0.72719	± 6
	biotite								440.7	6.624	202.8	1.25178	± 76
RS43/99	whole rock	0.421	0.727	0.3503	0.512474	± 8	-3.2	7.6E+8					
	garnet1	1.940	1.336	0.8780	0.513264	± 5							
	garnet2	1.418	0.571	1.5029	0.51414	± 10							
	muscovite	0.103	0.203	0.3058	0.5129	± 3							
RS64/99	whole rock	1.458	4.475	0.1970	0.512189	± 8	-8.8	5.6E+9					
	garnet	5.163	0.560	5.5850	0.522347	± 85							
	tourmaline	0.175	0.656	0.1615	0.512099	± 7							
RS35/00	feldspar	0.024	0.070	0.2087	0.512339	± 20			325.7	269.4	3.505	0.72656	± 4
	garnet	1.880	0.211	5.405	0.521206	± 12							
	muscovite								691.9	2.578	9.369	2.8317	± 7
RS11/00	whole rock								160.1	114.6	4.053	0.73764	± 6
	biotite								477.4	5.260	2.84.3	1.5488	± 35
RS13/00	whole rock	0.310	0.754	0.2487	0.512430	± 8	-5.6	4.0E+9					
	garnet	0.699	0.735	0.5756	0.512971	± 9							
B72c	whole rock	8.258	48.32	0.1033	0.511918	± 5	-14	1.5E+9					
	garnet	4.761	4.642	0.6201	0.513003	± 11							
G63	whole rock	0.446	0.958	0.2815	0.512275	± 7							
	garnet1	0.452	0.188	1.4571	0.514450	± 7							
	garnet2	0.309	0.132	1.4144	0.51416	± 24							

Table 2: Sm-Nd and Rb-Sr isotopic data from the samples presented in this paper.

and aligned to the dominant schistosity (D_o). It also forms millimetre-sized patchy pseudomorphs after garnet, which developed by the prograde breakdown of garnet by the reaction Grt + Ms = Sil + Bt + Qtz. Anatectic melting is indicated locally by neosome layers of Pl + Or + Qtz ± Bt ± Sil whereas plagioclase porphyroblasts are overgrowing the residual sillimanite-biotite schists. The neosom layers are concordant to the dominant schistosity which also deformes some pegmatites at temperatures of more than 500 °C.

Based on mineral assemblages, microfabrics and the deformation history two major metamorphic events can be identified in the Strieden Complex:

(1) In the garnet and staurolite-zone the first imprint is dominating. From the mineral assemblages upper greenschist facies conditions in the structural upper part and amphibolite facies conditions at medium pressures in the lower part can be expected. A Variscan age is indicated by a Sm-Nd garnet isochrone age of 342 ± 3 Ma (RS14/97; Fig. 4A) from the staurolite-garnet micaschists.

(2) The overprinting event shows HT/LP characteristics and a zonation with structural depth. In the uppermost part of the section features of the second imprint are scarce. Below

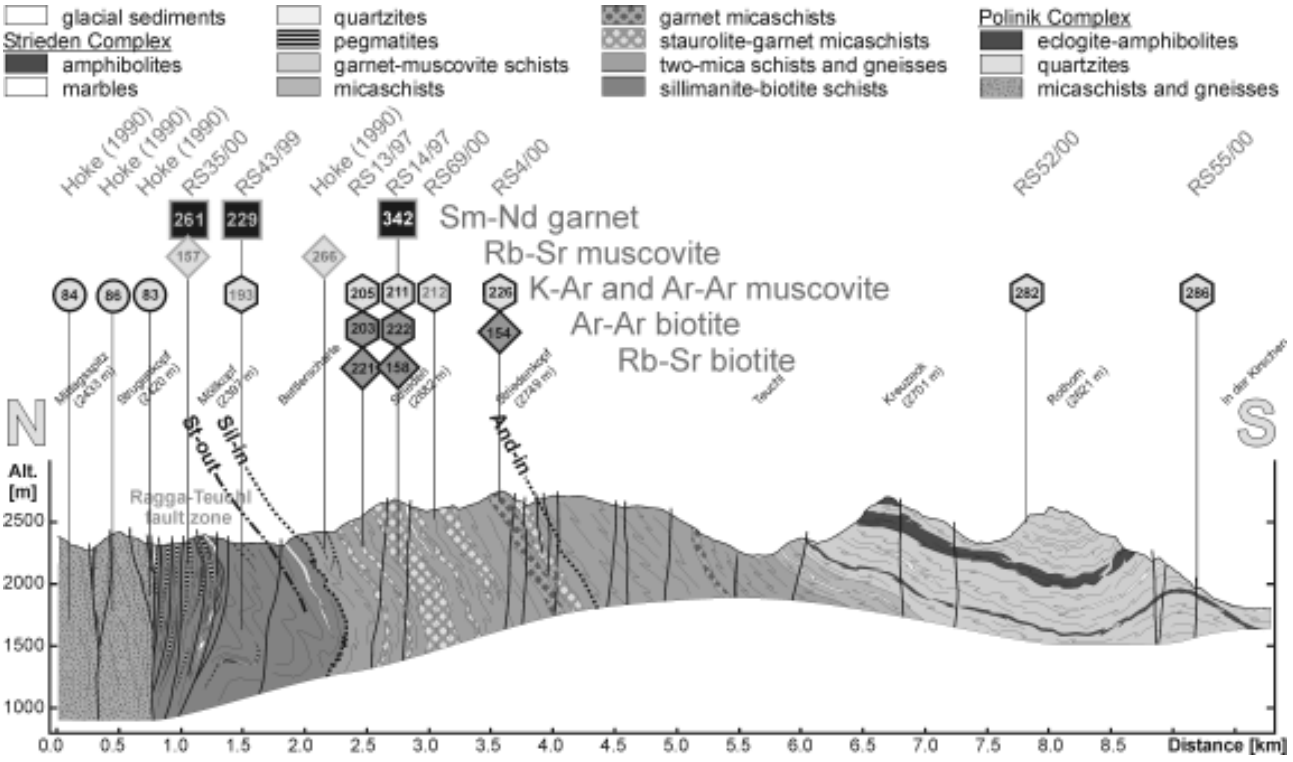

Fig. 2: Section through the Strieden Complex in the Kreuzeck Mountains. The Eo-Alpine eclogite-bearing Polinik Complex to the north is separated from the Strieden Complex by the Tertiary Ragga-Teuchl fault zone, which represents a segment of the SAM. The Strieden Complex is dipping to the south. From bottom to the top a lower and upper sillimanite-zone and an andalusite-zone can be mapped.

the andalusite-zone, an upper sillimanite-zone and a lower sillimanite-zone with partial anatexis developed. Pegmatites are obviously related to this thermal event because they occur only in the lowermost andalusite-zone and within the sillimanite-zone. The timing of the HT/LP event is defined by Sm-Nd garnet isochrone ages on magmatic garnets from a weakly deformed and a deformed pegmatite. Calculated with orthoclase and the whole rock they yielded well defined Permo-Triassic isochrone ages of 261 ± 3 Ma (RS35/00; Fig.4B) and 229 ± 3 Ma (RS43/99; Fig. 4C). Based on the breakdown of staurolite in the andalusite stability field conditions of c. 550 ± 50 °C at 0.35 ± 0.1 GPa can be expected for the andalusite-zone. For the lower sillimanite-zone temperatures of 650 ± 50 °C at pressures of 0.45 ± 0.1 GPa are indicated by the occurrence of anatectic mobilisates and the breakdown of garnet (see chapter 5.1.3.).

The cooling history of the rock pile was investigated by K-Ar, Ar-Ar and Rb-Sr ages on muscovites and biotites: K-Ar ages (BREWER 1970) and Ar-Ar plateau ages on muscovites exhibit Variscan ages (RS7/00: 316 ± 4 Ma; RS8/00: 311 ± 3 Ma; RS24/00: 312 ± 3 Ma) from the Goldeck and Gaugen Complexes below the transgressive Permo-Mesozoic Drauzug sediments and decrease with structural depth. In the Strieden Complex Ar-Ar muscovite ages of 286 ± 2 Ma (RS55/99) and 286 ± 3 Ma (RS52/99) were determined from garnet-muscovite schists. Staurolite-garnet micaschists yielded 226 ± 3 Ma (RS4/00) and 210 ± 2 Ma (RS14/97), whereas 212 ± 2 Ma (RS69/00) and 205 ± 2 Ma (RS13/97) have been measured for the andalusite-zone. The lowest age of 191 ± 2 Ma (RS43/00) has been found in the sillimanite-zone (Fig. 4E - 4L). Rb-Sr biotite-whole rock ages yielded 150 Ma to 225 Ma. These ages indicate tem-

Fig. 3: Lithologies of Austroalpine units south of the SAM. Indices of the minerals correspond to the time of their formation: V…Variscan, P…Permian, A…Alpine. A) Grt-Ms schist from the upper part of the Strieden Complex: syndeformative, Variscan garnet within a matrix of Ms + Chl + Qtz + Ilm. The pressure shaddows exist of quartz and chlorite (RS55/99; parallel Nicols). B) St-Grt micaschist from the upper part of the Strieden Complex: Variscan staurolite porphyroblasts in a matrix of Ms + Bt + Qtz + Pl + Ilm (RS14/97; parallel Nicols). C) And-Bt schist of the Strieden Complex: Relics of Variscan staurolite within a Permian andalusite porphyroblast (RS25/99; parallel Nicols). D) And-Bt schist of the Strieden Complex: Permian andalusite and plagioclase overgrowing a pre-existing microfabric defined by graphitic pigment and ilmenite (RS13/97; parallel Nicols). E) St-Sil schist from the upper sillimanite-zone of the Strieden Complex: Variscan staurolite porphyroblasts and biotite-sillimanite aggregates within a matrix of Ms + Pl + Qtz + Ilm (RS27/99; parallel Nicols). F) Sil-Bt schist of the Deferegger Alps: Variscan garnet relic intergrown with quartz within an aggregate of sillimanite and biotite (RS14/00; parallel Nicols). G) Garnet-bearing pegmatite Deferegger Alps: magmatic garnet, unduloes plagioclase and orthoclase within deformed quartz (RS13/00; perpendicular Nicols). H) Grt-St-And-Bt schist of the Jenig Complex: euhedral garnet and staurolite overgrown by Permian andalusite and biotite (RS9/98; parallel Nicols).

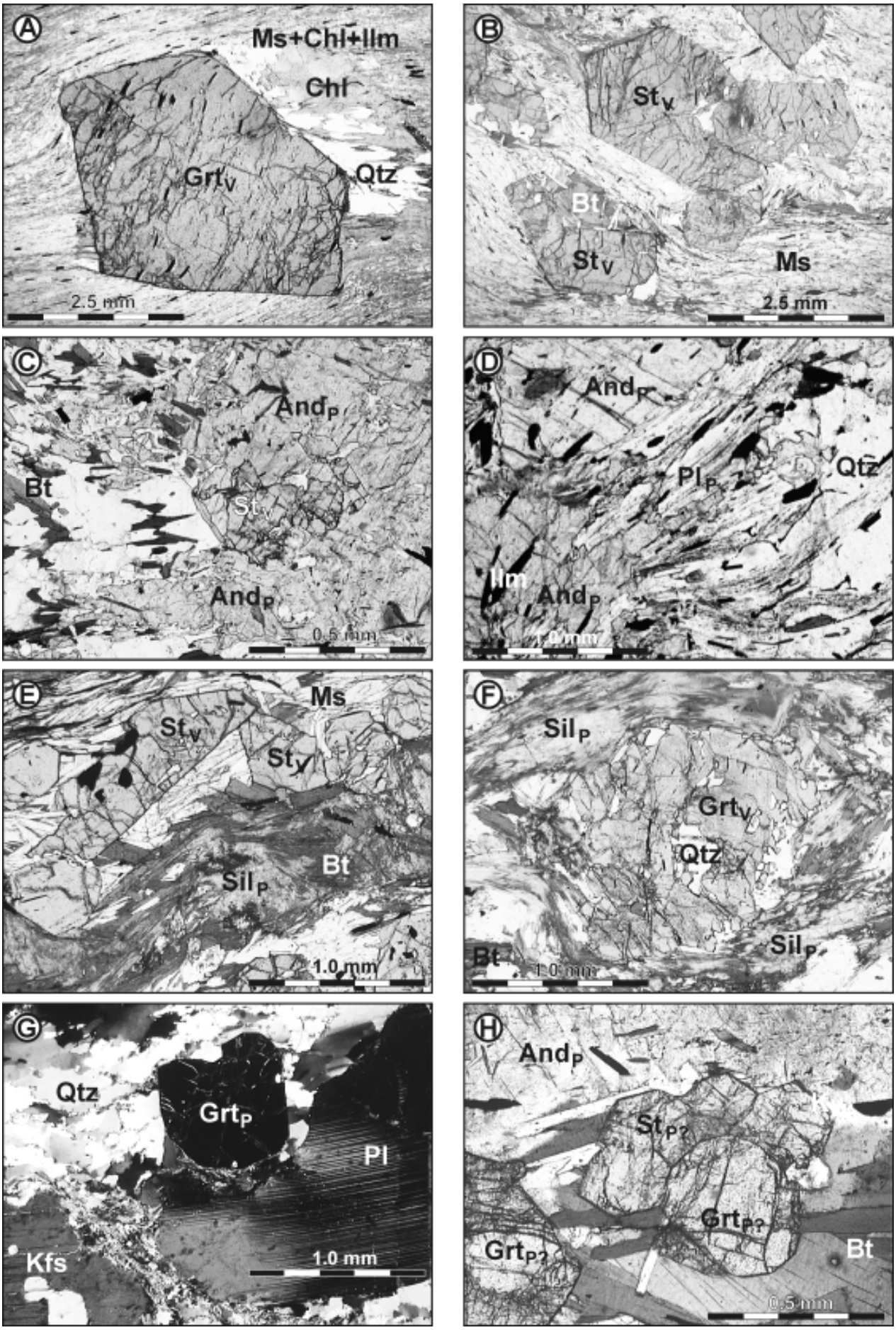
A
Ms+Chl+Ilm
Chl
Grt$_V$
Qtz
2.5 mm
B
St$_V$
Bt
St$_V$
Ms
2.5 mm
C
And$_P$
Bt
St$_V$
And$_P$
0.5 mm
D
And$_P$
Pl$_P$
Qtz
Ilm
And$_P$
E
Ms
St$_V$
St$_V$
Bt
Sil$_P$
1.0 mm
F
Sil$_P$
Grt$_V$
Qtz
Bt
Sil$_P$
1.0 mm
G
Qtz
Grt$_P$
Pl
Kfs
1.0 mm
H
And$_P$
St$_{P?}$
Grt$_{P?}$
Grt$_{P?}$
Bt
0.5 mm

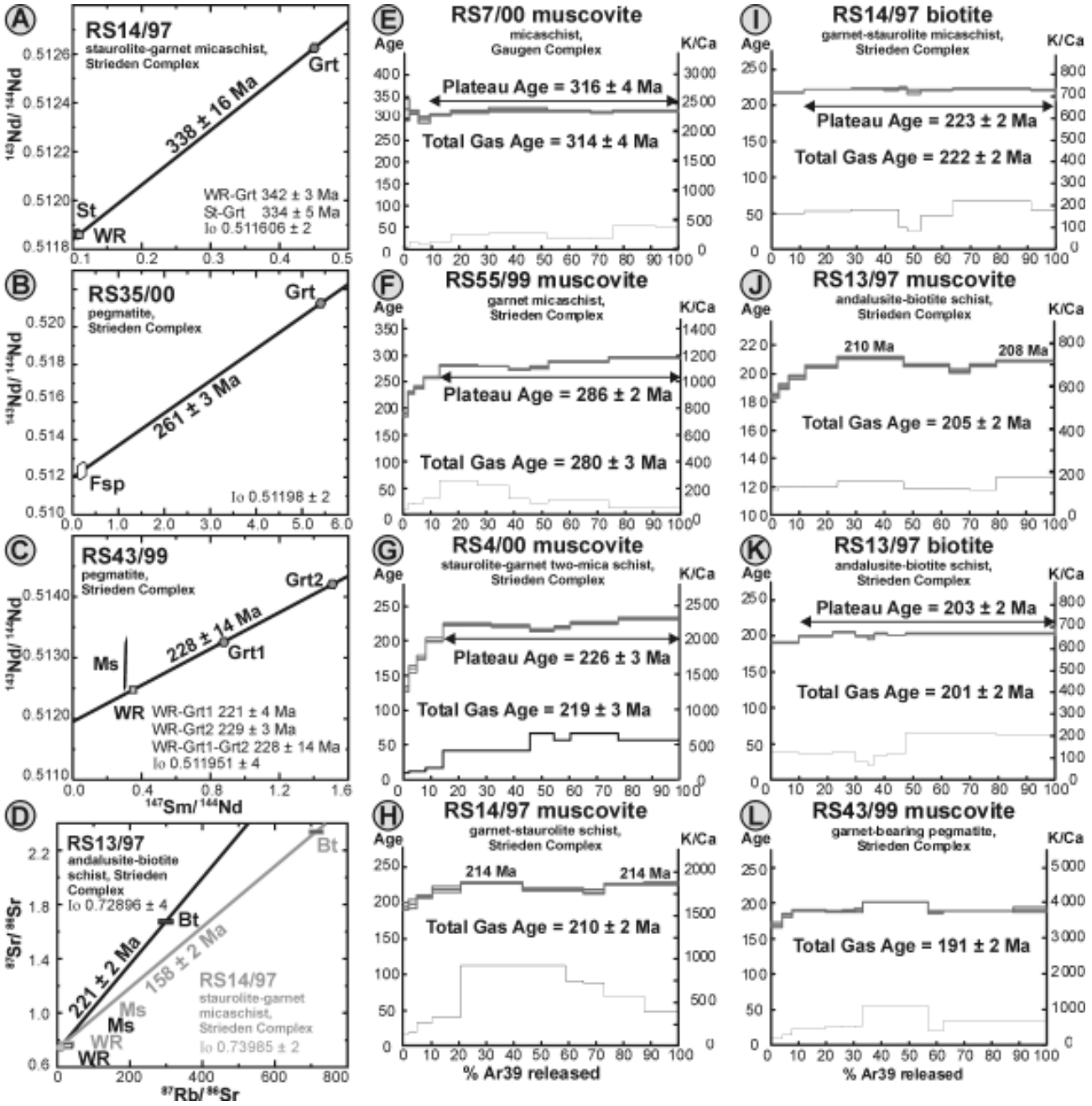

Fig. 4: Sm-Nd, Rb-Sr and Ar-Ar age diagrams on metamorphic rocks of the Strieden Complex. The ages reflect a Variscan metamorphic imprint overprinted by a medium to high-grade Permo-Triassic event.

peratures below 300 °C during the Alpine overprints (Fig. 4D)

In the **Defereggen Alps (2)** and in the **Uttenheim area** to the west two Austroalpine blocks can be distinguished (STÖCKHERT 1987). The one south of the SAM (represented by the Oligocene Defereggen–Antholz–Vals Line) shows many similarities to the andalusite and sillimanite-zone of the Strieden Complex. The structurally deepest parts consist of sillimanite-bearing biotite schists and biotite-plagioclase gneisses with intercalations of pegmatites, amphibolites and marbles (SENARCLENS-GRANCY 1972). In the metapelites sillimanite is intergrown with biotite and aligned to the dominant schistosity of the rocks. It also forms millimetre-sized patchy pseudomorphs after garnet, indicative of prograde breakdown of garnet by the reaction Grt + Ms = Sil + Bt + Qtz (Fig. 3F). The pegmatites are mostly concordant and have a magmatic mineral assemblage of Grt + Tur + Kfs + Pl + Qtz + Ms (Fig. 3G). They exhibit ductile deformation of the feldspars at more than 500 °C. Above the sillimanite-zone, fine-grained biotite-plagioclase gneisses with intercalations of staurolite and/or garnet-rich micaschists occur (SCHULZ et al. 2001). Andalusite has been observed as porphyroblasts within the micaschists and within crosscutting andalusite-quartz veins. The upper part of the unit is formed by garnet-micaschists, orthogneisses and phyllitic micaschists.

The pegmatites from the Uttenheim area have been inter-

preted as partial anatectic melts from the residual sillimanite-biotite schists. They formed during a HT/LP event at 650 ± 30 °C and 0.6 ± 0.1 GPa (STÖCKHERT 1987). A Rb-Sr whole rock isochrone of 262 ± 7 Ma (BORSI et al. 1980) and a Sm-Nd garnet isochrone age of 253 ± 7 Ma (RS13/00; Fig. 5A) have been determined for pegmatites from the Uttenheim area and from the Deferegger Alps. These ages indicate a Permian age for the pegmatites and for the contemporaneous HT/LP event. Ar-Ar ages on muscovites from a pegmatite and the surrounding sillimanite-biotite schist yielded 190 ± 3 Ma and 193 ± 2 Ma (RS11/00) (Fig. 5B and 5C). These ages represent cooling of the sillimanite-bearing rocks below 400 °C. The Rb-Sr isochrone age of biotite from the metapelite sample is 204 ± 2 Ma (Fig. 5D). As the closure temperature for the Rb-Sr isotopic system in biotite is expected to be c. 300 °C and as the age was not totally reset during the Alpine times Alpine temperatures did not exceed 300 °C.

Andalusite-bearing assemblages of the **Jenig Complex (3)** occur in a hundred metre wide tectonic lamella just north of the PAL (PHILLIPITSCH et al. 1986). The andalusite-bearing lithologies are graphitic, Al-rich metapelites with low XMg (0.20 – 0.23) and an assemblage of Grt + St + And + Bt + Ms + Chl + Pl + Ilm. They are intercalated andalusite-quartz veins and occur as layers within quartz-rich micaschists composed of Ms + Qtz + Chl + Bt.

Andalusite is overgrowing euhedral garnet and staurolite of unknown age (Fig. 3H). It formed by the reactions Chl + Ms = And + Bt + Qtz + H_2O and Pg + Qtz = Ab + And + H_2O at upper greenschist facies conditions. Based on the NKFMASH grid (SPEAR 1993) the P-T conditions for the andalusite formation can be estimated to be c. 570 °C at less than 0.4 GPa (see chapter 5.1.3.). Ar-Ar cooling ages on white mica and biotite (Fig. 5E, 5F, 5H, 5I) are in the range of 206 to 181 Ma. Rb-Sr ages of biotite (corrected with the whole rock) are 190 and 169 Ma (Fig. 5G). These ages reflect Triassic to Jurassic cooling of the rocks and an Alpine thermal overprint below 300 °C.

To the west the Variscan part of the **Meran-Mauls Basement (4)** (SPIESS 1995) is located between the PAL to the southeast and the SAM to the west and north (represented by the Passeier Jaufen Line). The northern part is composed of paragneisses and micaschists whereas in the south biotite-rich sillimanite-bearing gneisses and pegmatites occur. Rb-Sr as well as K-Ar ages on mica are in the range of 66 to 326 Ma, those of biotites yielded 78 Ma to 251 Ma (SATIR

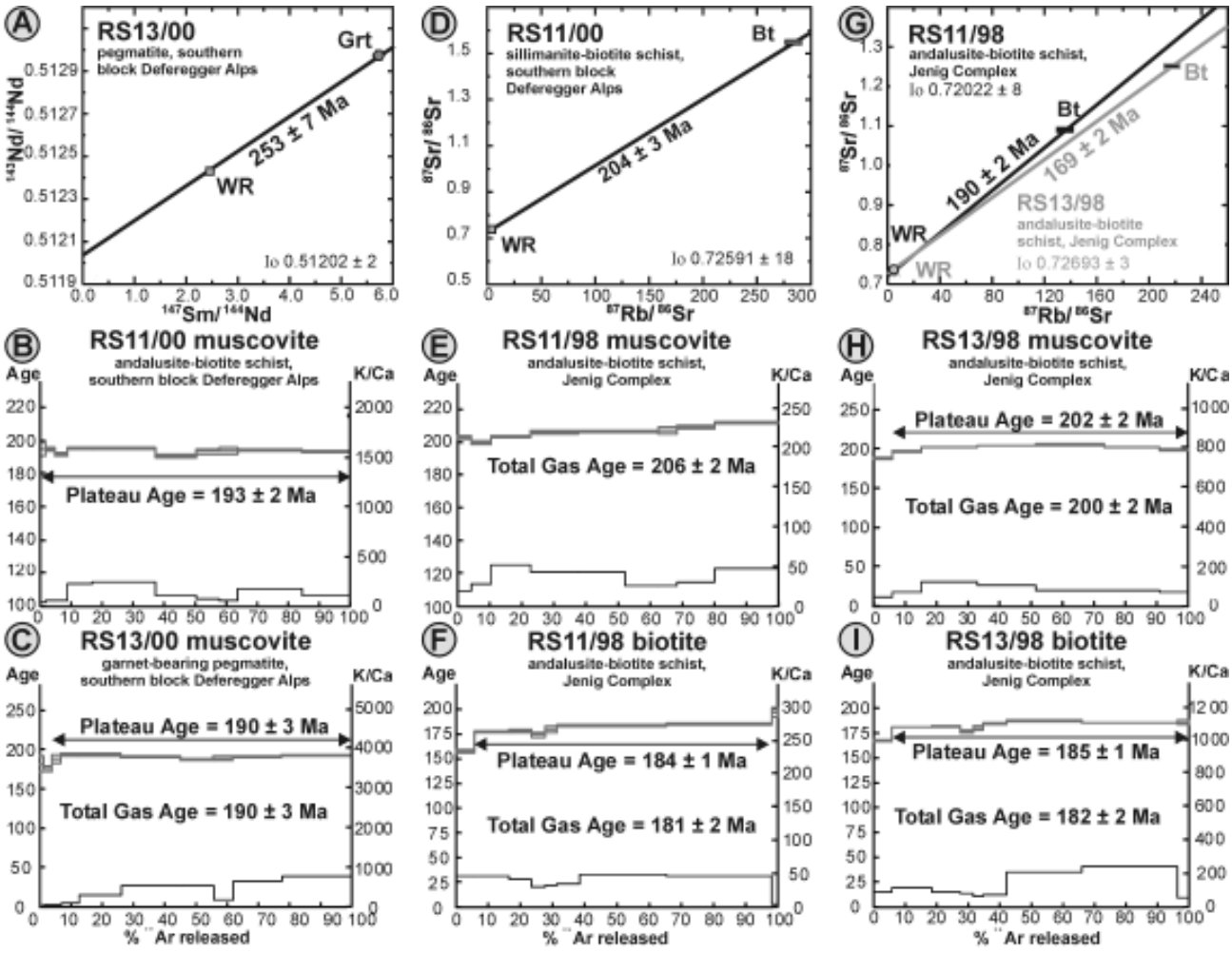

Fig. 5: Geochronological age data of metamorphic rocks from the Jenig Complex and the southern block of the Deferegger Alps.

1975, THÖNI 1983, SPIESS 1995). These ages have been interpreted as Variscan cooling ages partly reset during an Eo-Alpine overprint. However, facing the age zonation in the Strieden Complex an additional Permo-Triassic imprint seems to be likely. The only preserved Variscan ages of 305 and 326 Ma are Rb-Sr muscovite ages which represent cooling below c. 500 °C. Except one age of 66 Ma all Ar-Ar muscovite ages are in the range of 207 to 271 Ma and most of the biotite ages range from 140 to 251 Ma. As the latter are not totally reset during the Alpine overprint temperatures did not exceed 300 °C during this time. Therefore the Ar-Ar muscovite ages most probably represent Permo-Triassic cooling ages. Temperatures of the Permo-Triassic event caused a total reset of the K-Ar system but did not influence the Rb-Sr isotopic system of the muscovites. This indicates temperatures of 400 to 500 °C.

The **Eisenkappel intrusive Complex (5)** consists of gabbros, diorites, granodiorites and granites, which intruded into a Palaeozoic diabase and greenschist facies metamorphic metasediments (EXNER 1972, BOLE et al. 2001). A Permian age of 260 ± 19 Ma was determined for a gabbro (THÖNI, 1999), whereas a U/Pb age on titanite from a diorite is 230 ± 5 Ma (LIPPOLT & PIDGEON 1974). K-Ar cooling ages on hornblende are about 245 Ma, K-Ar and Rb-Sr data on biotite are in the range of 227 to 216 Ma (LIPPOLT & PIDGEON 1974, CLIFF et al. 1974, SCHARBERT 1975). From the existing data the Eisenkappel intrusive Complex can be interpreted as a Permo-Triassic intrusion, which cooled down during Triassic times within the upper crust.

The **Tonale Series (6)** forms a narrow zone between the SAM, represented by the Pejo and Mortirolo Lines to the north and the PAL (Insubric Line) to the south (WERNIG 1992). It is composed of high-grade sillimanite-bearing gneisses and micaschists, garnet and biotite-bearing amphibolites and marbles. As Permian granitoides, diorites and pegmatites are characteristic (DEL MORO et al. 1981) a contemporaneous Permo-Triassic age for the metamorphic imprint can be expected.

4.2. Austroalpine Units north of the SAM and west of the Gurktal Nappe System (7)

The Austroalpine crystalline units north of the SAM show a different Eo-Alpine metamorphic overprint. In the area west of the Gurktal Nappe System the metamorphic grades are decreasing from bottom to the top within the units and the regional pattern shows a decrease to the west and north respectively (HOINKES et al. 1999).

The **Silvretta Nappe (8)** represents a thrust sheet composed of crystalline basement, which is locally transgressed by Carboniferous clastic sediments and by the widely developed Permo-Triassic sedimentary cover of the Ducan and Langwasser synclines (29) and the Northern Calcareous Alps (30). It holds a northern position in the western part of the Austroalpine.
Literature with important implications for this study and/or geochronological cooling ages exist from HOERNES (1971), GRAUERT (1969), THÖNI (1981), KRECZY (1981), AMMAN (1985), FLISCH (1986) and SPIESS (1987). Based on the literature pegmatites postdating the Variscan structures occur along the eastern limit of the unit. They are embedded within sillimanite-bearing gneisses and micaschists. Sillimanite in this eastern part is younger than Variscan kyanite, postkinematic with respect to the Variscan deformation and growing by the breakdown of pre-existing garnet and staurolite (AMMAN 1985). For the southern part of the Silvretta Nappe BENCIOLINI (1994) proposed a Permian metamorphic imprint at 550 ± 50 °C and 0.4 ± 0.1 GPa which is contemporaneous to the formation of andalusite-quartz veins and extensional structures. At present no reliable formation ages of the pegmatites are available. Ductile deformation of magmatic feldspars indicates deformation at temperatures of more than 500 °C. K-Ar cooling ages of muscovites from the pegmatites and the surrounding schists are 144, 160, 174, 184, 199 and 207 Ma. New Ar-Ar ages yielded 191 ± 2 and 189 ± 2 Ma. Towards tectonically higher levels in the north and west, no more pegmatites can be observed and the K-Ar and Ar-Ar cooling ages are increasing. For example northwest of Galtür an Ar-Ar plateau age of 246 ± 2 Ma was determined on an orthogneiss muscovite. However data of this zone are scarce. Ar-Ar ages on muscovites and Rb-Sr ages on biotites from the crystalline basement below the transgressional contacts yield Variscan cooling ages of about 310 ± 5 Ma respectively 290 ± 15 Ma.
Until now geochronological ages below 280 Ma have been interpreted as Variscan ages partly reset by an Alpine overprint. Several arguments argue against this interpretation: If the muscovite K-Ar and Ar-Ar ages represent Alpine overprinted ages stepwise pattern with low-temperature ages close to the overprinting event would be expected. However even the Triassic and Jurassic Ar-Ar cooling ages exhibit plateau-type pattern without steps of Alpine ages (< 100 Ma). On the other hand if the Ar-Ar system of the muscovites were partially reset, temperatures close to 400 °C, would be indicated for the Alpine overprint. In this case totally or nearly totally reset Rb-Sr biotite ages would be expected because of the lower closure temperature of c. 300 °C for this isotopic system. However even the lowest ages are above 120 Ma.
Based on this data the Silvretta Nappe represents a crustal block with a prominent Variscan structural and metamorphic imprint (e.g. GRAUERT 1969, HOERNES 1971) which experienced a HT/LP overprint at an elevated geothermal gradient during Permo-Triassic times. At middle crustal levels sillimanite-bearing assemblages developed and pegmatites were emplaced. Subsequent cooling to the steady state geotherm produced a characteristic pattern of Ar-Ar muscovite ages. They are c. 190 Ma in the sillimanite-zone and increase up to 310 Ma below the Permo-Triassic sediments. The Alpine temperatures did not exceed 400 °C and were most probable just below 300 °C in the main parts of the Silvretta Nappe.

In the **Languard Campo Nappe (9)** granitoides, diorites, gabbros and pegmatites occur within low to medium grade muscovite-, biotite- and minor staurolite-bearing gneisses and micaschists with interlayered amphibolites, marbles and

quartzites (e.g. GAZZOLA et al. 2000). A Permian crystallisation age of c. 290 Ma was determined by Sm-Nd mineral isochrones for the Sondalo gabbroic complex (TRIBUZIO et al. 1999). Next, close to the gabbro complex there are many small granitic bodies, which yielded Rb-Sr muscovite ages ranging from 281 to 259 Ma. The country rocks are amphibolite facies sillimanite-bearing paragneisses with common amphibolite bands and rare marble layers. The Languard Campo Nappe was affected by an Eo-Alpine overprint of upper greenschist to amphibolite facies conditions (GAZZOLA et al. 2000).

The Marteller granite intrudes medium-grade metamorphic rocks of the **Ortler Campo Nappe (10)** (BOCKEMÜHL 1988). It is characterised by a magmatic mineral assemblage of Kfs + Pl + Qtz + Ms ± Tur ± Grt, whereas biotite is scarce. The inhomogeneous intrusive body consists of aplitic and pegmatitic rock types and is surrounded by an extensive swarm of deformed and undeformed dykes. Based on Rb-Sr data the age of the Marteller granite is 271 ± 3 Ma (BOCKEMÜHL 1988).

The **Matsch Nappe (11)** consists of polyphase metamorphic gneisses, micaschists, amphibolites, marbles and frequent pegmatites. The micaschists are characterised by assemblages of And + fibrolitic Sil + Bt + Pl + Ms + Qtz in the western part. Andalusite developed at the expense of Variscan staurolite by the reaction St + Ms + Qtz = And + Bt + H_2O. Fibrolitic sillimanite is present within shear bands. In the eastern area sillimanite is the only aluminumsilicate phase (GREGNANIN 1980, HAAS 1985). There, garnets are only preserved as relics enclosed by quartz, within aggregates of sillimanite and biotite. These microfabrics indicate the breakdown of the Variscan garnet by the reaction Grt + Ms = Sil + Bt + Qtz. A Rb-Sr whole rock isochrone of 290 ± 17 Ma was determined by HAAS (1985) for pegmatites of the Matsch Nappe. With respect to the observations in the Strieden Complex a contemporaneous, Permo-Triassic formation of the pegmatites and the HT/LP assemblages can be expected. The Eo-Alpine overprint reached lower greenschist facies conditions in the western part of the unit, whereas upper greenschist facies conditions are indicated by the formation of an Eo-Alpine garnet generation in the eastern segment.

The **Innsbruck Quartzphyllite Zone (12)** is located north of the Penninic Tauern Window. It consists of polymetamorphic greenschist facies phyllites and micaschists, which are intercalated by acidic subvolcanic orthogneisses. For the orthogneisses a Permian monazite U-Th-Pb-elektron micro probe (EMP)-age of 280 ± 25 Ma was determined (ROCKENSCHAUB et al. 1999). Ar-Ar and Rb-Sr muscovite ages are in the range of 206 to 268 Ma. As several texturally and chemically different mica generations can be distinguished, the age scatter is explained by a little component of Eo-Alpine phengite in those mica concentrates that yielded the lower values. The older ages are interpreted to reflect a Permo-Triassic low-grade metamorphic imprint at about 270 Ma (ROCKENSCHAUB et al. 1999).

sample	mineral	Rb [ppm]	Sr [ppm]	$^{87}Rb/^{86}Sr$	$^{87}Sr/^{86}Sr$	$2\sigma m$
Wölz1	whole rock			2.15	0.7251	± 1
Wölz2	whole rock			3.33	0.7295	± 1
Wölz3	whole rock			11.7	0.7558	± 1
Wölz4	whole rock			23.6	0.8021	± 1
Wölz5	whole rock			32.8	0.8275	± 1
31/83	whole rock	91.6	12.9	20.79	0.799	± 1
32/83	whole rock	169	68.0	7.25	0.77004	± 6
33/83	whole rock	100.9	87.9	3.35	0.76076	± 8
34/83	whole rock	156	70.0	6.50	0.77283	± 13
35/83	whole rock	105	70.8	4.32	0.76327	± 6
	muscovite	1115	11.94	295	1.62446	± 41
	albite	4.78	93.8	0.148	0.75413	± 10
36/83	whole rock	231	9.30	74.0	0.97011	± 10
37/83	whole rock	102	57.2	5.18	0.75043	± 10
38/83	whole rock	115	14.8	22.79	0.83555	± 10
39/83	whole rock	96.0	9.56	29.52	0.84132	± 10
40/83	whole rock	150	13.6	32.34	0.85088	± 10
	albite	6.70	6.19	3.17	0.80248	± 10
	muscovite	1028	1.81	2805.0	7.869	± 1
41/83	whole rock	82.9	88.5	2.731	0.75247	± 10
	orthoclase	4.23	155	0.080	0.74430	± 4
	muscovite	716	20.5	105	1.06210	± 7
42/83	whole rock	55.3	19.9	8.12	0.76477	± 10
43/83	whole rock	139	22	18.40	0.795	± 1
	muscovite	700	26.9	77.92	1.0323	± 1
44/83	whole rock	49.9	36.5	3.99	0.74120	± 10
45/83	whole rock	17.6	81.4	0.629	0.72920	± 10
46/83	whole rock	79.7	64.6	3.59	0.74428	± 10
47/83	biotite	103	80.0	3.76	0.73960	± 10
	muscovite fg.	243	197	3.59	0.73822	± 25
	muscovite cg.	240	186	3.75	0.73823	± 19
	biotite	575	6.19	275	0.92436	± 16
48/83	biotite	182	107.7	4.92	0.74387	± 10
49/83	whole rock	350	32.6	31.61	0.85831	± 15
	feldspar	816	31.5	77.45	0.98856	± 14
	muscovite	1475	4.01	1752.0	7.2084	± 21
50/83	whole rock	344	29.9	42.70	0.95351	± 21
51/83	whole rock	754	37.6	59.72	0.96503	± 15
52/83	whole rock	387	33.4	34.34	0.92264	± 12
53/83	whole rock	92.9	37.0	7.31	0.74123	± 10
54/83	whole rock	117	32.2	10.5	0.744	± 1
55/83	whole rock	101.4	31.0	9.53	0.74639	± 10
56/83	whole rock	81.2	31.8	7.48	0.73934	± 10
57/83	whole rock	172	52.4	9.58	0.75020	± 10
	feldspar	375	108	10.10	0.75143	± 9
	muscovite	583	11.9	145	0.96900	± 38
AB9	whole rock	360	38	28	0.82075	± 14
	muscovite	1036	3.7	1104	4.34490	± 10
AB10	whole rock	295	71	12.1	0.76416	± 12
	muscovite	702	9.22	239	1.54785	± 10
	biotite	1641	4.2	1267	1.94200	± 10

Table 3: Rb-Sr isotopic data from pegmatites of the Millstatt Complex (Millstätter Seenrücken, Carinthia).

sample	unit	lithology	mineral	Sm-Nd [Ma]	Rb-Sr [Ma]	Ar-Ar Plateau age [Ma]	Ar-Ar Total gas age [Ma]	inverse isochrone correl. age [Ma]	correlation factor
RS13/97	Strieden C.	And-Bt schist	muscovite				205 ± 2		
			biotite		221 ± 3	203 ± 2	201 ± 2	205 ± 2	0.52
RS14/97	Strieden C.	Grt-St micaschist	garnet	342 ± 3					
			muscovite			211 ± 2	210 ± 2	212 ± 2	0.77
			biotite		158 ± 2	223 ± 2	222 ± 2	223 ± 2	0.91
RS43/99	Strieden C.	pegmatite	garnet	229 ± 3					
			muscovite				191 ± 2		
RS52/99	Strieden C.	Grt-Ms schist	muscovite			282 ± 3	280 ± 3		
RS55/99	Strieden C.	Grt-Ms schist	muscovite			286 ± 2	280 ± 3		
RS4/00	Strieden C.	Grt-St micaschist	muscovite			226 ± 3	219 ± 3		
RS35/00	Strieden C.	Grt pegmatite	garnet	261 ± 3					
			muscovite		159 ± 2				
RS69/00	Strieden C.	And-Qtz-Ms vein	muscovite			212 ± 2	211 ± 2		
RS7/00	Gaugen C.	micaschist	muscovite			316 ± 4	314 ± 4		
RS11/00	Deferegger A.	Sil-Bt schist	biotite		204 ± 3				
			muscovite			193 ± 2			
RS13/00	Deferegger A.	Grt pegmatite	garnet	253 ± 7					
			muscovite			190 ± 2			
RS11/98	Jenig C.	And-Bt schist	muscovite				206 ± 2		
			biotite		190 ± 2	184 ± 1	181 ± 2	185 ± 4	0.18
RS13/98	Jenig C.	And-Bt schist	muscovite		169 ± 2	202 ± 2	200 ± 2	206 ± 4	0.41
			biotite			185 ± 1	182 ± 1	187 ± 2	0.45
RS22/96	Millstatt C.	pegmatite	muscovite		292 ± 3				
36-40/83	Millstatt C.	pegmatite	whole rock		215 ± 59				
41-48/83	Millstatt C.	pegmatite	whole rock		260 ± 75				
31-57/83	Millstatt C.	pegmatite	whole rock		286 ± 35				
40/83	Millstatt C.	pegmatite	muscovite		178 ± 13				
41/83	Millstatt C.	pegmatite	muscovite		213 ± 13				
43/83	Millstatt C.	pegmatite	muscovite		280 ± 4				
49/83	Millstatt C.	pegmatite	muscovite		259 ± 6				
57/83	Millstatt C.	pegmatite	muscovite		114 ± 7				
Ab9	Strallegg C.	pegmatite	muscovite		230 ± 2				
Ab10	Strallegg C.	granite	muscovite		243 ± 3				
RS1/95	Rappold C.	Grt pegmatite	garnet	262 ± 2					
RS8/95	Rappold C.	Grt-St micaschist	garnet	286 ± 3					
RS10/95	Rappold C.	pegmatite	muscovite		241 ± 3				
RS15/96	Rappold C.	pegmatite	muscovite		205 ± 2				
RS16/96	Rappold C.	pegmatite	muscovite		232 ± 3				
RS64/00	Rappold C.	Grt pegmatite	garnet	288 ± 4					
Wölz 1-5	Rappold C.	pegmatite	whole rock		240 ± 23				
G63	Sau-Koralpe C.	Grt micaschist	garnet	267 ± 17					

Table 4: Geochronological age data from the samples presented in this paper.

For the Eo-Alpine eclogite and/or amphibolite facies metamorphic units along the SAM less informations on the pre-Alpine metamorphic history is available. However pegmatites of presumed Permian age are known from the Laas Serie, the northern unit of the Deferegger Alps, the Schober Mountains and the Polinik Complex in the Kreuzeck Mountains. Several Permian and Triassic Rb-Sr isotopic data of pegmatites, partly influenced by the Eo-Alpine overprint exist for the **Millstatt Complex (13)** (Fig. 6A - 6D, Table 4).

4.3. Austroalpine Units north of the SAM and east of the Gurktal Nappe System

In the east of the Gurktal Nappe System the Austroalpine crystalline units form a nappe stack which formed during the exhumation of the Eo-Alpine high-pressure metamorphic rocks. In the northern part an increasing metamorphic imprint to structural higher units in the south can be observed (DALLMEYER et al. 1998, HOINKES et al. 1999, SCHUSTER & FRANK 2000). In this chapter two sections are described.

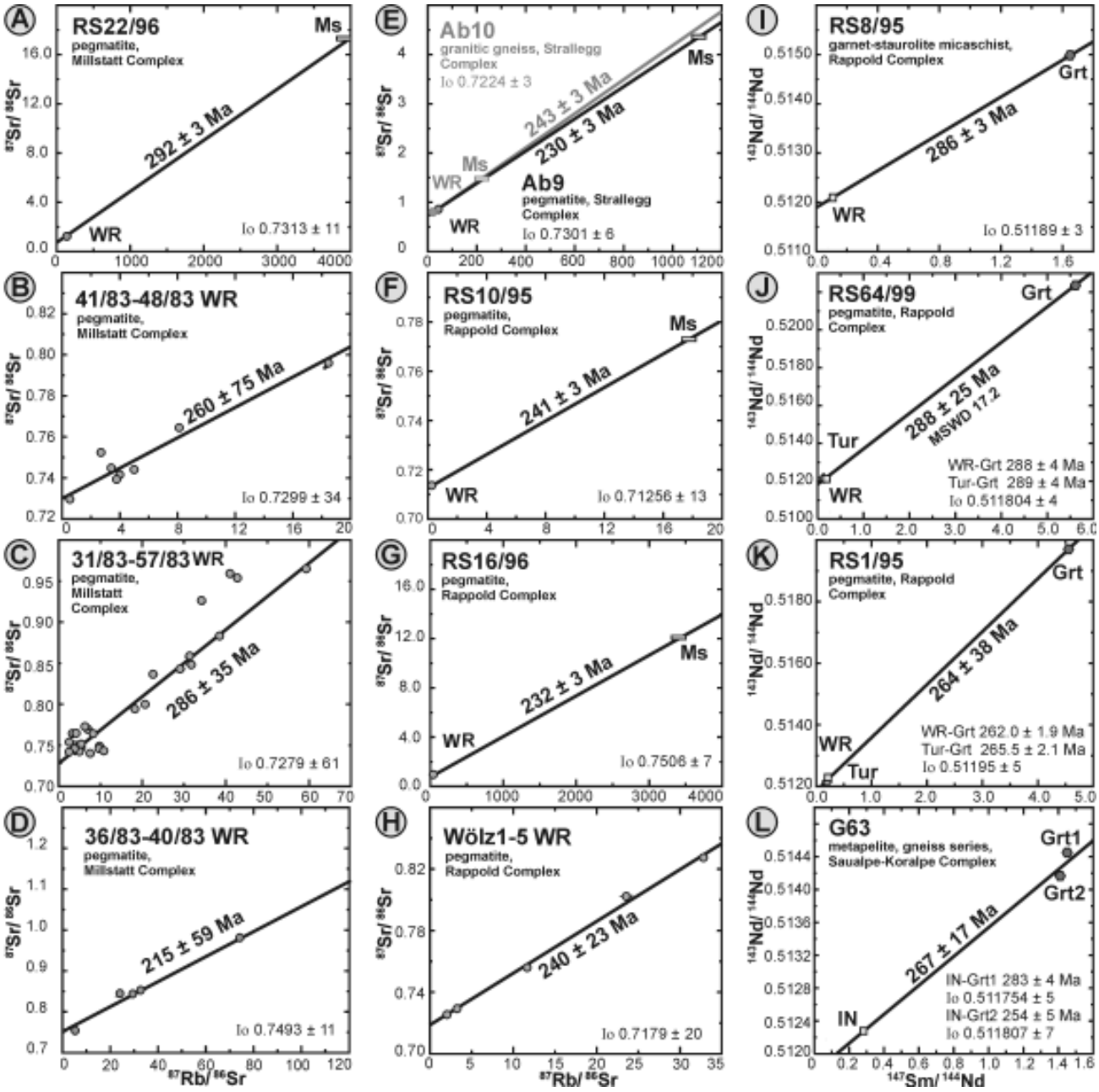

Fig. 6: Sm-Nd and Rb-Sr age data from the Strallegg, Wölz, Rappold and Saualpe-Koralpe Complexes.

The first section covers the easternmost part of the Eastern Alps and comprises from bottom to the top the Wechsel, Semmering, Strallegg and Sieggraben Complexes. A detailed description of this succession is available in SCHUSTER et al. (2001a) and therefore only a brief summary is given here.

The **Wechsel Complex (14)** is mainly composed of gneisses and structurally overlying phyllitic micaschists. MÜLLER et al. (1999) published geochronological ages of paragonitic mica which yielded c. 245 Ma and interpreted them as indications for a Permo-Triassic lower greenschist facies metamorphic imprint.

The tectonically overlying **Semmering Complex (15)** exhibits a southward increase of the metamorphic grade which might be due to internal thrusting. Permo-Triassic metasediments and Permian quartzporphyric volcanic rocks are overlying phyllitic rocks of the northernmost Semmering Complex (GAAL 1966). Lazulite-quartz veins crosscutting the phyllites are dated at 246 ± 23 Ma by the U-Th-Pb EMP method on xenotime (BERNHARD et al. 1998). They argue for a hydrothermal event in the northernmost part of the unit. The main part of the Semmering Complex consists of polyphase metasediments with huge masses of porphyric orthogneisses. The latter are associated with small gabbro bodies. Recently a crystallisation age of 264 ± 7 Ma was determined for a gabbro by the Sm-Nd method and zircon ages in the same range are reported for the orthogneisses from the same area (PUMHÖSL et al. submitted). As the gabbros and granites intruded at an original depth of c. 15 km a contemporaneous metamorphic imprint of the coun-

try rocks can be expected.

The **Strallegg Complex (16)** on top of the Semmering Complex is composed of polyphase metamorphic, biotite-rich micaschists and migmatic gneisses with scarce amphibolite intercalations. Typically granites, orthogneisses and pegmatites are intercalated. The Strallegg Complex is of special interest, because in the northernmost occurrences pre-Alpine andalusite and sillimanite-bearing lithologies are locally well preserved, whereas in the south their Eo-Alpine transformation into kyanite-rich gneisses can be studied. The microfabrics of the aluminumsilicate-bearing lithologies are complex. The oldest relics are cores of polyphase garnets and resorbed staurolites within younger andalusite porphyroblasts (Fig. 7A). The garnet cores yielded a Sm-Nd crystallisation age of 321 ± 2 Ma which indicates a Variscan medium-grade metamorphic imprint (BERKA 2000, SCHUSTER et al. 2001a).
During a HT/LP overprint medium to high-grade assemblages including Sil, Crd, And, Bt and Kfs developed (LELKES-FELVÀRI & SASSI 1984, DRAGANITS1998, TÖRÖK 1999, BERKA 2000). Based on observations from TÖRÖK (1999) two sillimanite generations occur: the older developed by the breakdown of paragonitic mica by the reaction Pg + Qtz = Sil + Ab + H_2O at 550 - 600 °C and 0.32 – 0.48 GPa. This sillimanite is present as inclusions within andalusite. Andalusite formed by the reaction St + Ms + Qtz = And + Bt + H_2O at lower pressures. A younger sillimanite occures within extensional shear bands and between boudinaged andalusite porphyroblasts (Fig. 7B). Metamorphic peak conditions reached 640 – 710 °C at 0.22 – 3.8 GPa (DRAGANITS 1998, TÖROK 1999, BERKA 2000). The granites and pegmatites represent synmetamorphic intrusions with respect to the HT/LP event. They are crosscutting the schistosity defined by the HT/LP assemblages, but they are also deformed by synmetamorphic structures. The age of the HT/LP imprint is defined by Sm-Nd garnet isochrone ages of metasedimentary and magmatic rocks which yielded 276 ± 4 Ma, 263 ± 3 Ma, 286 ± 3 Ma. Several Rb-Sr whole rock and muscovite isochrones (Fig. 6E) and U-Th-Pb EMP ages on monazites are in the same range (SCHARBERT 1990, BERNHARD et al. 2000, BERKA 2000, SCHUSTER et al. 2001a). These data prove a Permo-Triassic age for the HT/LP imprint.
The Eo-Alpine metamorphic event reached conditions of 450 - 550 °C at 0.8 – 1.3 GPa in the northern part of the Strallegg Complex (MOINE 1989, DRAGANITS 1998, TÖRÖK 1999). This overprint caused the formation of complex pseudomorphs after andalusite and sillimanite composed of Ky, Cld, Crn, St, Pg and Mrg. In the south conditions of 530 – 600 °C at 1.2 – 1.5 GPa have been determined by TROPPER et al. (2001). There the alumosilicates were transformed into kyanite aggregates (Fig. 7C and 7D) (DRAGANITS 1998, TÖRÖK 1999, BERKA 2000). These kyanite pseudomorphs exhibit fine-grained internal textures reminding of ice crystals on window glasses (Fig. 7E). Affected by deformation they form irregular patches, sometimes surrounded by fine-grained muscovite (Fig. 7F).

Sieggraben Complex (17)
The Sieggraben Complex holds the uppermost tectonic position in the southeastern part of the nappe stack. It is composed of biotite-rich kyanite-bearing gneisses, metagabbros, eclogite-amphibolites, orthogneisses, pegmatite gneisses, marbles and serpentinites (KÜMEL 1935, MILOTA 1983). Due to an Eo-Alpine eclogite facies and subsequent amphibolite facies metamorphic imprint (NEUBAUER et al. 1999a, PUTIS et al. 2000) the pre-Alpine structures and assemblages are mostly destroyed. However, the presence of pegmatites and the kyanite pseudomorphs after andalusite and sillimanite indicate a Permo-Triassic metamorphic imprint.

The second section is located directly east of the Gurktal Nappe System. From bottom to the top it comprises the Wölz, Rappold, Saualpe-Koralpe and Plankogel Complexes.

The **Wölz Complex (18)** forms a thrust sheet composed of partly graphitic, garnet-bearing micaschists with intercalations of paragonite-amphibolites and scarce marble and quartzite layers. Microtextures in the major part of the unit indicate one prograde metamorphic imprint at upper greenschist in the north and epidote-amphibolite facies conditions in the south (SCHUSTER & FRANK 2000). However in several localities garnet porphyroblasts (Fig. 7G) with optically and chemically distinct cores (Grt_P) and younger rims (Grt_A) occur. The cores are idiomorphic, have a pinkish colour and contain monomineralic inclusions of Mrg, Pg, Ms, Ep, Qtz, Ilm and Tur. The core of one garnet yielded a well defined Sm-Nd crystallisation age of 269 ± 4 Ma (SCHUSTER & THÖNI 1996, SCHUSTER & FRANK 2000) and hence a Permian age of formation. The chemical zoning patterns and the mineral inclusions of the garnet cores indi-

Fig. 7: Lithologies of Austroalpine units north of the SAM. Indices of the minerals correspond to the time of their formation: V…Variscan, P…Permian, A…Alpine. A) And-Bt schist from the northern Strallegg Complex: relics of Variscan staurolite within a Permian andalusite porphyroblast (RS7/96; parallel Nicols). B) same sample: sillimanite growing between boudinaged andalusite porphyroblasts (RS7/96, parallel Nicols. C) same sample: replacement of Permian andalusite by fine-grained Eo-Alpine kyanite along the edges and within cracks of the andalusite (RS7/96, parallel Nicols). D) Ky-bearing gneiss from the Strallegg Complex: Eo-Alpine kyanite pseudomorph after Permian sillimanite within a matrix of biotite, plagioclase and quartz (RS10/97; parallel Nicols). E) Ky-bearing gneiss from the Saualpe-Koralpe Complex: Kyanite pseudomorph after chiastolitic andalusite. (RS3/96; parallel Nicols). F) Ky-bearing micaschist from the southern Strallegg Complex: Eo-Alpine, fine-grained kyanite pseudomorph after Permian andalusite. The kyanite is partly replaced by muscovite (RS9/97; parallel Nicols). G) Garnet micaschist from the Wölz Complex: polyphase garnet with a Permian core and an Eo-Alpine rim (RS44/97; parallel Nicols). H) Grt-St-Ky micaschist from the Rappold Complex: Permian assemblage including garnet, staurolite and andalusite overprinted by the Eo-Alpine event. Andalusite is replaced by Eo-Alpine, fine-grained kyanite. Eo-Alpine garnet and staurolite are present (RS51/97; parallel Nicols).

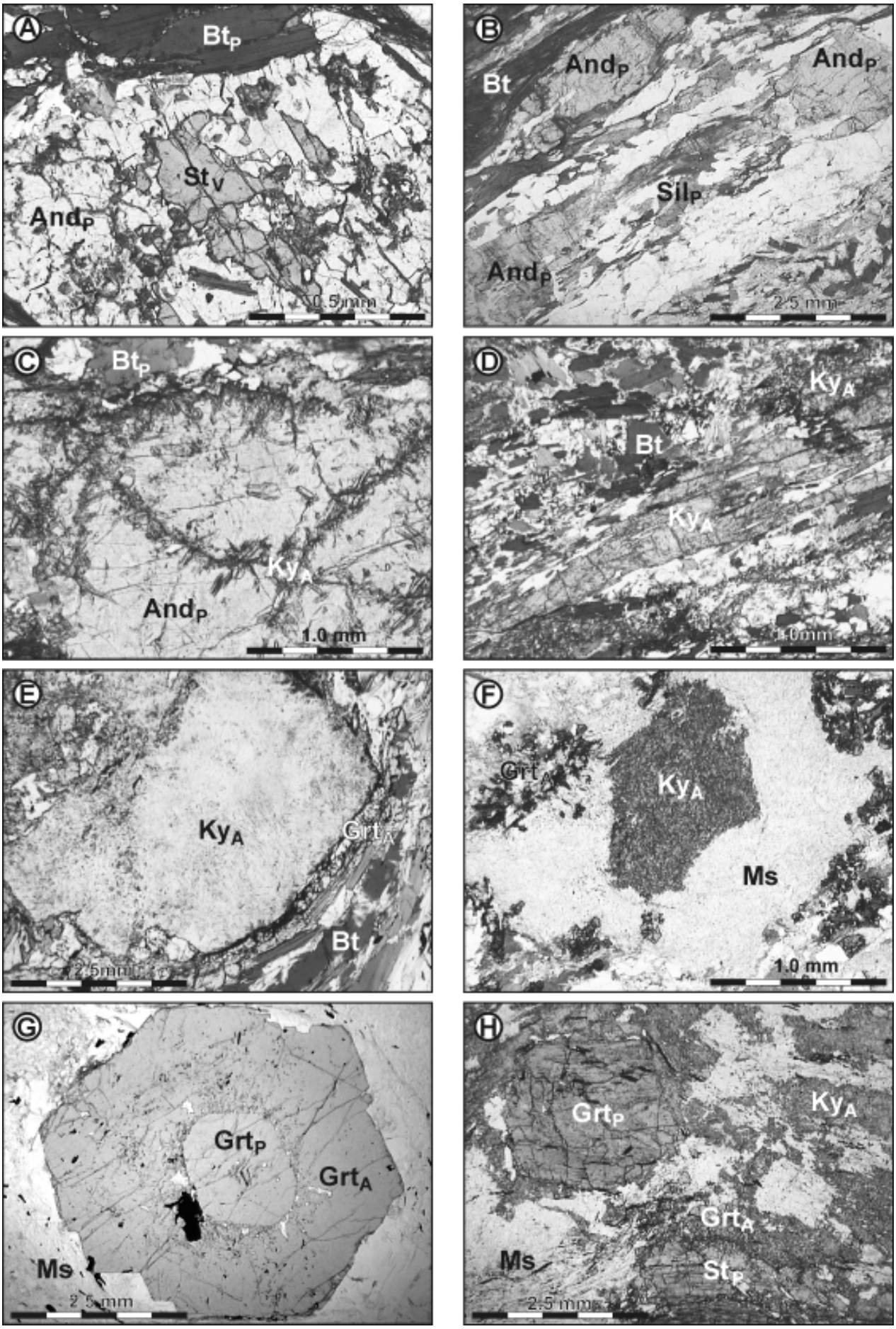
A
Bt$_P$
St$_V$
And$_P$
0.5 mm
B
And$_P$
Bt
And$_P$
Sil$_P$
And$_P$
2.5 mm
C
Bt$_P$
Ky$_A$
And$_P$
1.0 mm
D
Ky$_A$
Bt
Ky$_A$
1.0 mm
E
Ky$_A$
Grt$_A$
Bt
2.5 mm
F
Grt$_A$
Ky$_A$
Ms
1.0 mm
G
Grt$_P$
Grt$_A$
Ms
2.5 mm
H
Grt$_P$
Ky$_A$
Grt$_A$
Ms
St$_P$
2.5 mm

cate upper greenschist facies conditions and low pressures during their growth. An Eo-Alpine age of the dominating metamorphic event of the Wölz Complex is proved by numerous geochronological age data (SCHUSTER & FRANK 2000).

In the tectonically overlying **Rappold Complex (19)** graphitic garnet and staurolite-bearing micaschists with complex polymetamorphic mineral assemblages are dominating. In contrast to the Wölz Complex amphibolites are scarce, whereas marbles and pegmatites are typical. From the microfabrics two amphibolite facies assemblages can be distinguished: (1) The older one is defined by a mineral association including large staurolite (St_p) and garnet (Grt_p) porphyroblasts (Fig. 7H) and a mineral phase which has been transformed into fine-grained kyanite later on. With respect to the Strallegg Complex these aggregates are interpreted as former andalusite crystals. (2) The second assemblage consists of St_A + Grt_A + Ky + Ms + Bt + Pl + Qtz. St_A and Grt_A are present as tiny euhedral crystals in the matrix. Grt2 forms rims around Grt1, and together with kyanite also around St_p. The latter developed by the prograde breakdown of St_p by the reaction St_p + Ms + Qtz = Ky + Grt + H_2O. Kyanite is also present as larger porphyroblasts. A Sm-Nd garnet isochrone of a garnet core (Grt_p) calculated with the whole rock yielded a well defined Permian age of 286 ± 3 Ma (RS8/95; Fig. 6I). Sm-Nd ages of intercalated pegmatite veins, calculated from magmatic garnet, tourmaline and the whole rock yielded 288 ± 4 Ma (RS64/99; Fig. 6J) and 262 ± 2 Ma (RS1/95; Fig. 6K). Rb-Sr muscovites ages of pegmatites corrected with the whole rocks scatter between 205 Ma and 240 Ma (Fig. 6F - 6H). These data indicate a Permian formation of the older amphibolite facies imprint, which occurred at low pressures in the andalusite stability field and during the emplacment of the pegmatites. The overprinting event is Eo-Alpine in age (HOINKES et al. 1999, THÖNI 1999) and reached temperatures up to 650 °C (LICHEM et al. 1996).

The **Saualpe-Koralpe Complex (20)** is a polymetamorphic unit with a complex internal structure. It consists of various micaschists and kyanite-bearing paragneisses with intercalated marbles, eclogites and amphibolites. Rocks of magmatic origin are metagabbros, pegmatite gneisses and the Wolfsberg granite-gneiss. The present day metamorphic and structural behaviour of the unit is the result of the Eo-Alpine tectonothermal event, which reached eclogite and subsequent amphibolite facies conditions (FRANK et al. 1983, THÖNI & JAGOUTZ 1992, MILLER & THÖNI 1997). Indications for the former geodynamic evolution of the unit have been determined by the magmatic rocks and locally preserved mineral relics from the metasedimentary rocks. Such mineral relics are pre-Alpine garnet cores or frequent kyanite pseudomorphs after andalusite like in the Strallegg Complex. The most impressive relics of a pre-eclogite facies HT/LP event are up to half a metre long kyanite pseudomorphs after chiastolithic andalusite within metapelites (Fig. 7E) (BECK-MANNAGETTA 1970) and idiomorphic kyanite pseudomorphs after andalusite from pre-existing andalusite-quartz veins. They occur in the southern part of the Koralpe.

Geochronological age data yielded Permian and Triassic crystallisation ages for the Wolfsberg granite-gneiss (MORAUF 1980), gabbroic rocks (MILLER & THÖNI 1997), metabasalts (HEEDE 1997) and for pegmatite gneisses (THÖNI & MILLER 2001). From the Saualpe HABLER & THÖNI (1998) calculated metamorphic conditions of 590 ± 20 °C at 0.38 ± 0.1 GPa for a contemporaneous HT/LP imprint. They used relic assemblages preserved within garnet cores from metapelites. A Sm-Nd isochrone from such a garnet core from the northernmost Saualpe yielded 267 ± 17 Ma (G63; Fig. 6L).

The **Plankogel Complex (21)** is overlying the Saualpe-Koralpe Complex in the south and the west with a normal fault contact (FRANK et al. 1983, HABLER 1999). It consists of graphitic garnet micaschists with minor marbles, Mn-quartzites and serpentinites. As in the Wölz Complex the centimetre-sized garnet porphyroblasts are characterised by distinct cores (Grt1) and younger rims (Grt2) (GREGUREK 1995). The garnet rims are part of an amphibolite facies mineral assemblage of Grt2 + St + Cld + Ky + Ms + Pg + Chl + Qtz. A Permian Sm-Nd isochrone age of c. 285 Ma has been determined for the cores of the garnets (LICHEM et al. 1997). The overprinting event in the kyanite stability field is Eo-Alpine in age (HOINKES et al. 1999).

The presented data document a Permo-Triassic metamorphic imprint in most of the Austroalpine units, from the easternmost outcrops near Sopron in Hungary to the Tonale Series in Italy over a distance of c. 500 km. It is characterised by HT/LP conditions that reached up to high amphibolite and granulite facies conditions. The best preserved successions, e.g. in the Drauzug-Goldeck-Kreuzeck or Silvretta areas, represent more or less continuous sections through the Permo-Triassic middle and upper crust. They show typical zonations of mineral assemblages, magmatic rocks and cooling ages. The same features can be found in truncated tectonic elements, which are segments of the complete sections. For example in the Matsch Nappe only the andalusite-zone and sillimanite-zone are preserved, representing a middle crustal level.
Crystalline units which show no indications of this imprint, e.g. the Ötztal (22), Gailtal, Schladming, Seckau-Rennfeld-Mugel-Troiseck (23) or Bundschuh Complexes (24) are transgressed by Permo-Triassic sedimentary piles. Therefore they stayed in a high tectonic position and the temperatures were too low to influence the isotopic systems we use to detect the thermal event. At a geothermal field gradient of 60 °C/km the blocking temperature of biotite (300 °C) was reached at 5 km depth. It can be concluded that the whole Austroalpine realm was affected by the Permo-Triassic thermal event.

5. Discussion

In the following discussion we try to give an interpretation on the geodynamic processes, which are responsible for the Permo-Triassic thermal event. The discussion comprises the following items: (1) At first the data from the Austroalpine

units are summarised to define typical features of the event. (2) The results are compared to existing data from the Southalpine realm and surrounding areas, which exhibit indications for a similar Permo-Triassic geodynamic evolution. (3) Based on the whole data set the thermal history and the geotectonic settings for the HT/LP metamorphism are deduced. (4) At last the plate tectonic environment is discussed in a wider palaeogeographic framework.

5.1. Typical features

In this chapter the field relations of the Permian and Triassic magmatic rocks to their metamorphic country rocks, the available P/T data and geochronological age data of the different units are compared, to find out if the same geodynamic processes where acting in the whole Austroalpine area.

5.1.1. Relations of magmatic and metamorphic rocks

Permo-Triassic magmatic rocks comprise pegmatites, gabbros, diorites, granites, and volcanic rocks. They are common but volumetrically subordinate with respect to the country rocks.

At least two types of pegmatites occur: (1) the majority is characterised by mineral assemblages of Or + Pl + Qtz + Ms + Tur ± Grt, (2) scarce spodumene-bearing pegmatites occur in the same areas, e.g. in the Deferegger Alps (Schuster et al. 2001b), as well as in the Strieden (Marsch 1983), Rappold and Saualpe-Koralpe Complexes (Thöni & Miller 2001). The spodumene-free pegmatites have strongly negative initial εNd (-5.7 - -16.3) values and high initial $^{86}Sr/^{87}Sr$ ratios (0.718-0.749), arguing for a crustal origin. They are interpreted as in-situ melts by partial mobilisation of the metasedimentary country rocks (Stöckhert 1987, Thöni & Miller 2001).

Important field relations can be determined in the units south of the SAM. Pegmatites are frequent in the sillimanite-zones, and occur up to the andalusite-zone in the Strieden Complex. This indicates amphibolite facies conditions at minimum temperatures of more than 550 °C during their emplacement. They exhibit ductile deformation and recrystallisation of the magmatic feldspars at more than 500 °C. As the Alpine metamorphic conditions reached lowermost greenschist facies in the areas south of the SAM the feldspars indicating synintrusive deformation.

Based on the distribution of the pegmatites south of the SAM, a Permo-Triassic metamorphism in the stability field of sillimanite or andalusite can be expected for those of the highly overprinted units north of the SAM, which contain pegmatites. Indeed in many places, e.g. the southern Strallegg, Saualpe-Koralpe or Sieggraben Complex they are associated with kyanite-bearing, biotite-rich gneisses, which are interpreted as former andalusite and/or sillimanite-bearing rocks.

The gabbros derived from different mantle sources. For example those from the Semmering Complex were generated from an enriched subcontinental mantle source (Pumhösl et al. submitted), whereas the Bärofen gabbro in the Saualpe-Koralpe Complex exhibits N-MORB characteristics (Miller & Thöni 1997). In several localities they are associated with diorites and/or granites, e.g. in the Languard Campo Nappe (Tribuzio et al. 1999), the Eisenkappel intrusive Complex (Exner 1972) or the Semmering Complex (Pumhösl et al. submitted).

The granites intruded into Permo-Triassic medium-grade crustal levels but they also occur in low-grade areas, e.g. the Eisenkappel intrusive Complex (Exner 1972) or the subvolcanic orthogneisses in the Innsbruck Quartzphyllite Zone (Rockenschaub et al. 1999). Lower Permian quartzporphyries reach the surface in the westernmost part of the Northern Calcareous Alps (Haditsch et al. 1979) on top of the Silvretta Complex, in the Drauzug on the Goldeck, Gaugen and Strieden Complexes as well as on the Semmering Complex (Gaal 1966) in the east.

Basic tuffs and volcanogenetic sediments occur as thin layers within the sedimentary piles of the Northern Calcareous Alps, in the Engadin Dolomites and in the Drau Range. From the latter area scarce lava flows are known. The volcanic activity is Anisian to Ladinian (227 ± 5 to 242 ± 5) in age and define a distinct magmatic event (Tollmann 1977, Obenholzner 1991).

5.1.2. Peak metamorphism and cooling history

About 200 geochronological age data establish the Permo-Triassic metamorphic event. They scatter in a wide range, from 300 to 190 Ma, because they were measured by different methods representing magmatic or metamorphic crystallisation ages, as well as cooling ages through different blocking temperatures.

However, magmatic and metamorphic crystallisation ages argue for a peak of the thermal event at 270 ± 30 Ma (Fig. 8A). The still large scatter of the data might be explained by a slightly different time of the thermal peak at different crustal levels and different localities. The available Rb-Sr data are in a range of 250 ± 50 Ma (Fig. 8B). As they include whole rock errorchrones and muscovite data and since the Rb-Sr isotopic system might be influenced by the Eo-Alpine event in some areas, the younger mean value and a broader scatter is understandable.

Of great interest is the zonation in the K-Ar and Ar-Ar muscovite ages, which show a correlation between the peak temperature and the time of cooling (Fig. 8C). In the best preserved sections the Ar-Ar ages yield Variscan cooling ages of c. 310 Ma in the uppermost kilometres below the Mesozoic cover series. Below age values of 260 to 280 Ma can be found. Going downward to structural deeper levels the ages are decreasing to c. 225 Ma just above the andalusite-zone, c. 210 Ma within the andalusite-zone and about 190 Ma in the sillimanite-zone. Taking into account the concept of closure temperature and the timing of the thermal peak at about 270 Ma, the following interpretation seems likely: within the uppermost kilometres below the transgressive surface the temperatures were below the closure temperature and the Variscan cooling ages of c. 310 Ma survived. At structural deeper levels c. 400 °C were reached during the temperature peak at about 270 Ma. The micas were reset, but closed immediately when the tem-

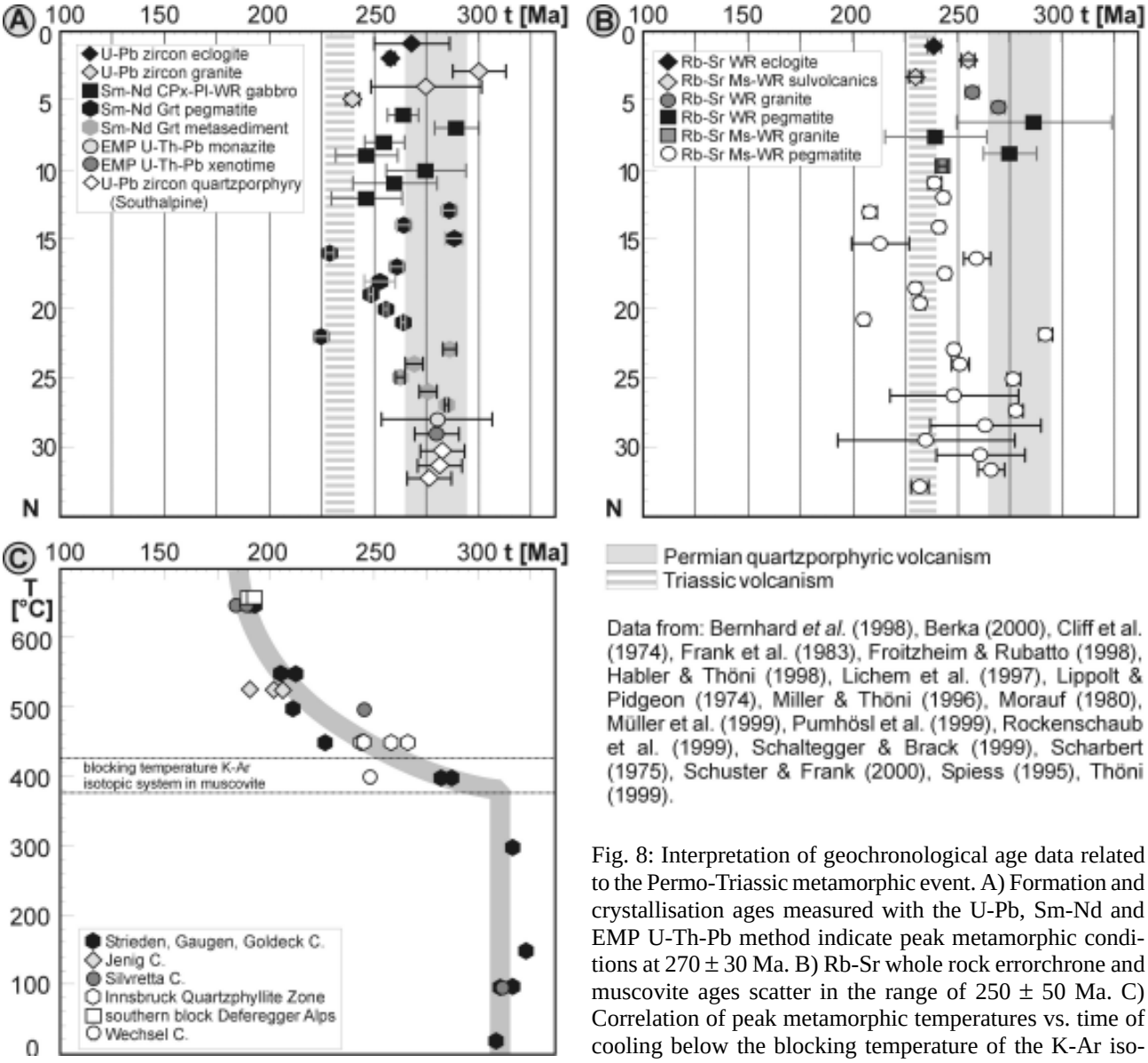

Data from: Bernhard *et al.* (1998), Berka (2000), Cliff et al. (1974), Frank et al. (1983), Froitzheim & Rubatto (1998), Habler & Thöni (1998), Lichem et al. (1997), Lippolt & Pidgeon (1974), Miller & Thöni (1996), Morauf (1980), Müller et al. (1999), Pumhösl et al. (1999), Rockenschaub et al. (1999), Schaltegger & Brack (1999), Scharbert (1975), Schuster & Frank (2000), Spiess (1995), Thöni (1999).

Fig. 8: Interpretation of geochronological age data related to the Permo-Triassic metamorphic event. A) Formation and crystallisation ages measured with the U-Pb, Sm-Nd and EMP U-Th-Pb method indicate peak metamorphic conditions at 270 ± 30 Ma. B) Rb-Sr whole rock errorchrone and muscovite ages scatter in the range of 250 ± 50 Ma. C) Correlation of peak metamorphic temperatures vs. time of cooling below the blocking temperature of the K-Ar isotopic system in muscovite (400 °C). The grey line shows the theoretically expected distribution of the age data.

peratures were decreasing. Going downward in the section the time gap between peak of metamorphism and the closure of the K-Ar isotopic system increased, because it took more time to cool rocks down from higher peak temperatures to the closure temperatures. Surprisingly very similar cooling ages can be found in many places. Andalusite-bearing rocks from the Strieden (205 ± 2 Ma, 212 ± 2 Ma) and Jenig Complexes (202 ± 2 Ma, 206 ± 2 Ma) yielded ages in a narrow range of about 205 Ma. Rocks from the sillimanite-zone of the Strieden Complex (193 ± 2 Ma), the Deferegger Alps (190 ± 2 Ma, 193 ± 2 Ma) and the Silvretta Complex (189 ± 2 Ma, 190 ± 2 Ma) cooled down at about 190 Ma.
Most of the K-Ar, Ar-Ar and Rb-Sr data of biotites are lower than those of the muscovites from the same samples. They are scattering due to the involvement of excess-Ar or the incomplete reset of the isotopic systems during the Alpine thermal overprints.

5.1.3. Metamorphic conditions

The Permo-Triassic metamorphic rock series show typical mineral assemblages and metamorphic reactions, which define a low-pressure trend from greenschist to granulite facies conditions (Fig. 9).
Greenschist facies rocks can be identified by the occurrence of Permian magmatic rocks and geochronological means (e.g. Innsbruck Quartzphyllite Zone, Wechsel Complex, Meran-Mauls Basement). The upper greenschist facies micaschists of the Wölz and Plankogel Complexes are characterised by their typical Permian garnet porphyroblasts. Due to Alpine overprints or insignificant mineral assemblages no quantitative P-T determinations are available for the low-grade metamorphic rocks at present.
Medium- and high-grade assemblages contain andalusite and/or sillimanite and are intercalated by pegmatites in most cases. Until now no Permo-Triassic garnet generation has been identified within the alumosilicate-bearing assem-

blages. For the andalusite formation the reactions Chl + Ms = And + Bt + Qtz + H_2O, Pg + Qtz = And + Ab + H_2O and St + Ms + Qtz = And + Bt + H_2O have been observed. In the Jenig Complex only the breakdown of chlorite and paragonite is visible. Based on the P-T grids metamorphic conditions of more than 570 °C at less than 0.4 GPa can be expected. The staurolite consuming reaction is typical for the Strieden and Strallegg Complexes and the Matsch Nappe. This reaction limits the pressure to less than 0.3 GPa at more than 600 °C and indicates a geothermal field gradient of more than 45 °C/km.

Sillimanite formed by the reactions Pg + Qtz = Sil + Ab + H_2O, Grt + Ms = Sil + Bt + Qtz and Ms + Qtz = Sil + Kfs + H_2O. The paragonite breakdown has been described from the Strallegg Complex (TÖRÖK 1999). Sillimanite produced by this reaction developed at 550 - 600 °C and 0.32 – 0.48 GPa and pre-dates the andalusite, because sillimanite is present as inclusions within andalusite. Also the plagioclase porphyroblasts, which are overgrowing the sillimanite-biotite schists of the lower sillimanite-zone of the Strieden Complex can be explained by this reaction. The consumption of garnet is observed in the Strieden and Silvretta Complexes, the Deferegger Alps and the Matsch Nappe. It occurs at pressures below 0.65 GPa and temperatures of more than 650 °C. The muscovite breakdown accompanies the formation of pegmatites and/or neosom layers in the Strieden, Silvretta and Strallegg Complexes. In the Strallegg Complex this sillimanite is younger than andalusite because it occures within extensional shear bands and between boudinaged andalusite porphyroblasts (Fig. 7B). Except in the Strallegg Complex no relics of cordierite have been found. Based on the P-T grids peak metamorphic conditions occurred at more than 640 – 710 °C and 0.22 – 3.8 GPa. The observed pressures indicate that the sillimanite-bearing lithologies have been situated at middle crustal depths of c. 15 km.

Conclusive is the occurrence of different sillimanite generations in the sillimanite-andalusite-biotite schists of the Strallegg Complex. The observed crystallisation sequence sillimanite-andalusite-sillimanite indicates a more or less isothermal decompression, followed by isobaric heating. The first part of this path has to be due to extension, the second part reflects advective heating.

Additional information on the thermal regime of the Austroalpine has been observed by thermal modelling of illite crystallinity and vitrinite reflection data for the sedimentary series in the north-westernmost part of the Austroalpine (FERREIRO MÄHLMANN & PETSCHICK 1996). The data argue for a geothermal field gradient of 55 to 70 °C/km for rocks close to the surface.

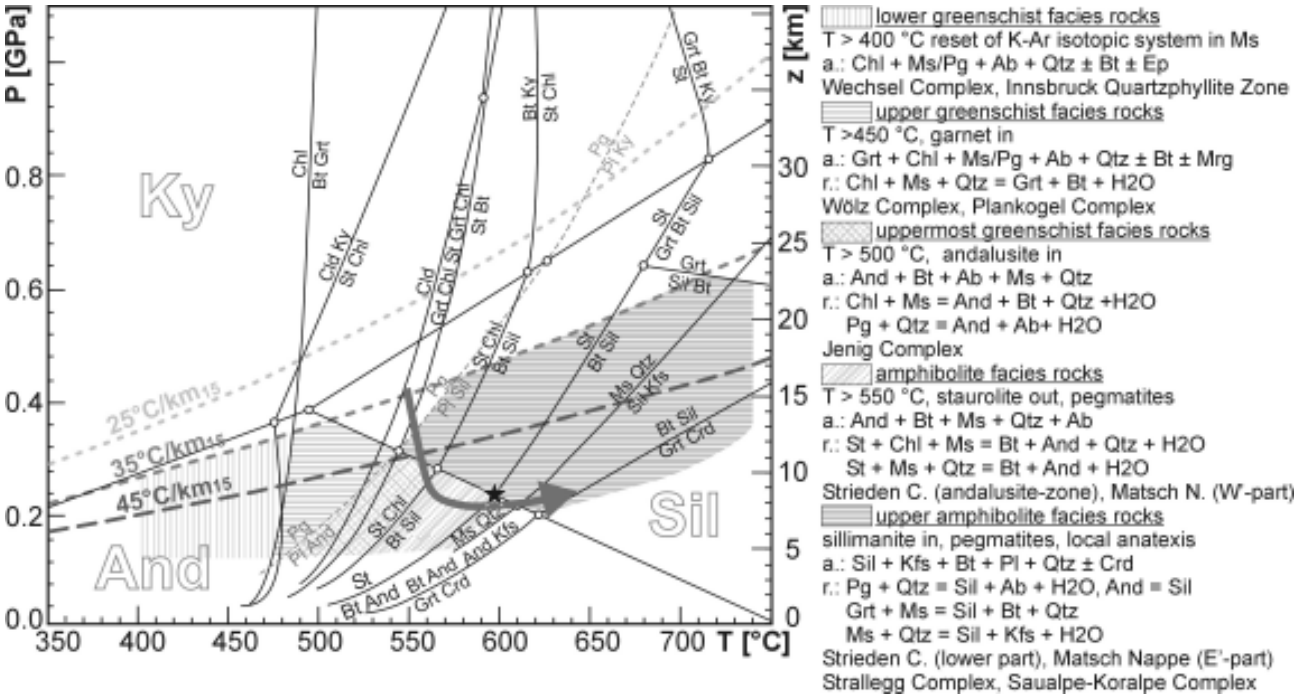

Fig. 9: Simplified P-T diagram showing metamorphic reactions in the KFMASH system and the paragonite breakdown reaction, assuming presence of quartz and mica in excess and water saturation (SPEAR 1993). Only curves identified from textural evidence and curves that limit the stability field of diagnostic mineral assemblages are shown. In the diagram geotherms for geothermal field gradients of 25, 35 and 45 °C/km (at 15 km depth) are shown. The P-T conditions for the various metamorphic units are based on observed index minerals and diagnostic assemblages (a.) and reactions (r.). The prograde breakdown of Variscan staurolite by the reaction St + Ms + Qtz = And + Bt + H_2O could be repeatedly identified. It implies, that the P-T path has to cross the andalusite = sillimanite univariant curve below the invariant point marked by the asterisk, indicating a geothermal field gradient of more than. 45 °C/km. The arrow shows the P-T path of the andalusite and sillimanite-bearing assemblages in the northern Strallegg Complex (TÖRÖK 1999).

Nr.	unit		T [°C]	P [GPa]	g [°C/km]	P*	mineral assemblage or index minerals	observed reaction/ method	reference
1	Strieden C.	garnet-zone	> 400				reset of K-Ar in muscovite		
		andalusite-zone	500 - 570	0.25 - 0.4	47 ± 13	P	And + Bt + Ms + Pl + Qtz	St + Ms + Qtz = And + Bt + H2O	Hoke (1990)
		sillimanite-zone	600 - 750	0.3 - 0.5	46 ± 18	P	Sil + Bt + Pl + Qtz, anatexis	Grt + Ms = Sil + Bt + Qtz + H2O	Hoke (1990)
2	Jenig Complex		450 - 550	0.2 - 0.4	46 ± 16		And + Bt + Ms + Pl + Qtz	Chl + Ms + Qtz = And + Bt + H2O	
3	Deferegger A.	andalusite-zone				P	And + Bt + Ms + Pl + Qtz		
		sillimanite-zone				P	Sil + Bt + Pl + Qtz	Grt + Ms = Sil + Bt + Qtz + H2O	
4	Meran-Mauls Basement		400-500	?		P	reset of K-Ar but not of Rb-Sr in muscovite		Spiess (1995)
6	Tonale Series					P	Sil + Bt + Pl + Qtz		Del Moro (1981)
8	Silvretta C.	E'- part				P	Sil + Bt + Pl + Qtz		
		S'-part	550 ± 50	0.4 ± 0.1	38 ± 11		And, Sil	Pl-Hb, Plyusnina (1982)	Benciolini (1994)
9	Languard-Campo Nappe		610 - 750	0.5 ± 0.1	37 ± 10		Sil + Opx + Kfs + Bt + Qtz		Giacomini et al. (1999)
10	Ortler-Campo Nappe		610 - 750	0.5 ± 0.1	37 ± 10		Sil + Opx + Kfs + Bt + Qtz		Giacomini et al. (1999)
11	Matsch Nappe	W'-part	c. 640	0.35 - 0.55	43 ± 10	P	And + Sil + Bt + Ms + Pl + Qtz	St + Ms + Qtz = And + Bt + H2O	Haas (1984)
		E'-part	570 - 600	0.3 - 0.45	39 ± 11	P	Sil + Bt + Ms + Pl + Qtz	Grt + Ms = Sil + Bt + Qtz	Haas (1984)
12	Innsbruck Quartzphyllite		300 - 450	?			Ms + Chl + Ab + Qtz		Rockenschaub et al. (1999)
13	Millstatt C.					P			
14	Wechsel C.		300 - 450	?			Pg + Chl + Ab + Qtz		Müller et al. (1999)
15	Semmering C.	N'-part					lazulite-quartz veins		Bernhard et al. (1998)
		S'-part					gabbros, granites		Pumhösl et al. (submitted)
16	Strallegg C.	NW'-part	c. 620	c. 0.35	49 ± 11	P	And + Sil + Bt + Ms + Pl + Qtz	St + Ms + Qtz = And + Bt + H2O	Berka (2000)
		NE'-part	c. 600	c. 0.35	51 ± 11	P	And + Sil + Bt + Ms + Pl + Qtz	St + Ms + Qtz = And + Bt + H2O	Draganits (1998)
		NE'-part	575 ± 50	0.4 ± 0.1	45 ± 10	P	And + Sil + Bt + Ms + Pl + Qtz	Pg + Qtz = Sil +Ab + H2O	Török (1999)
		NE'-part	650 ± 50	0.3 ± 0.1	60 ± 15	P	And + Sil + Bt + Ms + Pl + Qtz	Ms + Qtz = Sil +Kfs + H2O	Török (1999)
		S'-part	600 - 750	?		P	And + Sil + Bt + Ms + Pl + Qtz	anatexis	
17	Sieggraben C.					P	And, Sil		
18	Wölz Complex		440 - 520	0.2 - 0.4	48 ± 15		Grt, Mrg, Pg, Ep, Qtz		Schuster & Frank (2000)
19	Rappold Complex					P	And?, Grt		
20	Saualpe-Koralpe C.		590 ± 20	0.38 ± 0.1	43 ± 11	P	Grt + Sil + Bt + Pl + Ms + Qtz	Berman (1988), Hoisch (1991)	Habler & Thöni (1998)
21	Plankogel C.		> 450	?			Grt		Lichem et al. (1996)
25	Dervio-Oligasco Zone		640 - 750	0.4 - 0.55	43 ± 8	P	And + Sil + Bt + Ms + Pl + Qtz	Grt + Ms = Sil + Bt + Qtz + H2O	Diella et al. (1992)
26	Strona-Ceneri Z.					P	Sil, And, Crd		Boriani & Burlini (1995)
27	Ivrea Zone		730 ± 50	0.55 ± 0.1	27 ± 5	P	Sil + Bt + Grt + Kfs + Pl	Bt + Sil + Qtz = Grt + Kfs + H2O	Colombo & Tunesi (1999)
		granulite facies	850 + 100	0.85 ± 0.05	36 ± 9		Pl + CPx ± OPx ± Grt + Ilm ± Kfs		Colombo & Tunesi (1999)
		granulite facies	875 + 25	0.8 ± 0.02	31 ± 3		Pl + CPx ± OPx ± Grt + Ilm ± Kfs		Colombo & Tunesi (1999)
30	Northern Calcareous Alps		?	?	67 ± 12			vitrinite reflexion, illite crystallinity	Ferreiro Mählmann & Petschick (1996)

P* ... occurrence of pegmatites

Table 5: Permo-Triassic P-T data of rock series from the Austroalpine-Southalpine realm. Numbers refer to those in Fig. 1 and in the text. The errors on the average geothermal gradient (g) are calculated from maximum error on the temperature and pressure value.

5.2. Extension of the Permo-Triassic metamorphic event

As the Permo-Triassic event affected the whole Austroalpine unit, it can be expected also in those crustal blocks, which were neighbouring to the Austroalpine during this time. Based on palaeogeographic reconstructions (e.g. HAAS et al. 1994, STAMPFLI et al. 1998) these are the Southalpine realm, the Transdanubian Range, the Tisza Superunit, the Carpathian realm and the Helvetic and Penninic units respectively.

5.2.1. Southalpine

As mentioned in the introduction Permo-Triassic extension, metamorphism and magmatism has been recognised in the Southalpine earlier than in the Austroalpine realm. Permo-Mesozoic to Cenozoic sedimentary sequences form the larger part of the surface in the Southalpine realm (Fig. 1). The horst and graben structured basement, is outcropping along the PAL and shows successively deeper crustal levels from east to the west, as indicated by the increasing metamorphic grade of the basement rock series (VAI & COCOZZA 1986). All together a crustal section through the Permo-Triassic crust from the sediments down to the crust mantle boundary can be studied.
Based on the sedimentary record and the horst and graben structures an extensional environment is proved for the Southalpine unit during Permo-Triassic times. For the time between c. 225 and 160 Ma, BERTOTTI et al. (1993) was able to reconstruct the extension history of the Lombardian basin suggesting a total extension of $\delta = 1.22$.
In Anisian to Ladinian times the Southalpine domain was affected by explosive volcanism with regional scale tuff layers (Pietra verde) (OBENHOLZNER 1991). Magmatism culminated in the emplacement of several hundred metres thick volcanic deposits and the Monzoni intrusive Complex (c. 230 Ma; BORSI et al. 1968) in the central part of the unit (Dolomiten). Based on the chemical characteristics the volcanic event might be linked to regional transcurrent and/or transpressive tectonics (CASTELLARIN et al. 1987). Lower Permian quartzphorphyric volcanic rocks are typical in the Southalpine unit. They form ignimbrit layers within the clastic sediments of the graben structures and an up to 3000 m thick caldera structure in the area around Bozen. Based on U-Pb zircon data the quartzporphyries extruded in a narrow range at about 280 Ma (SCHALTEGGER & BRACK 1999). Lower Permian S-Type granitoides intruded into low and medium-grade metamorphic units below the volcanic rocks (e.g. Brixen, Iffinger, Monte Croce and Baveno intrusives) (ROTTURA et al. 1997, STÄHLE et al. 2001).
In the **Dervio-Olgiasca Zone (25)** medium to high-grade HT/LP assemblages are overprinting Variscan amphibolite facies rocks (DIELLA et al. 1992, SANDERS et al. 1996, BERTOTTI et al. 1999, DI PAOLA & SPALLA 2000). The Variscan assemblages include Grt + Bt + Qtz + St +Ky ± Pl + Ms ± Rt ± Ilm ± Tur. The overprinting event causes the breakdown of garnet by the reaction Grt + Ms = Sil + Bt + Qtz in the structurally lower part. Within the sillimanite-biotite schists anatectic pegmatites developed during the HT/LP imprint (SANDERS et al. 1996). In the structurally upper part (near to Corenno Plinio) andalusite is present as large porphyroblasts with inclusions of Qtz, Pl, Grt, St, Ky, Bt and Kfs (DIELLA et al. 1992). Metamorphic conditions (Fig. 10, Tab. 5) of 640 - 750 °C at 0.4 - 0.55 GPa have been determined for the HT/LP event for metapelites (DIELLA et al. 1992) as well as for amphibolites (DI PAOLA & SPALLA 2000). The timing of the metamorphic peak is not known at present, because no formation ages are available. A Permian age (≥ 240 Ma) was proposed by DIELLA et al. (1992), whereas a Triassic age (220 to 240 Ma) was favoured by BERTOTTI et al. (1999). The latter interpretation is based on Rb-Sr muscovite ages of the pegmatites (SANDERS et al. 1996), but the knowledge from the Austroalpine unit shows that these ages are too young in many cases. However, after the metamorphic peak isobaric cooling of the rocks can be recognised. Ar-Ar cooling ages on muscovites are 195 to 200 Ma (BERTOTTI et al. 1999).
A similar evolution is documented for the **Strona-Ceneri Zone (26)** (COLOMBO & TUNESI 1999). In its westernmost part rocks with sillimanite, andalusite and cordierite are associated with pegmatites and Permian mafic to intermediate intrusives (BORIANI & BURLINI 1995).
The **Ivrea Zone (27)** at the western end of the Southalpine contains mantle peridotites and an igneous complex, which intruded into lower crustal rocks in Permian times (COLOMBO & TUNESI 1999). The igneous complex is composed of predominantly gabbros and lesser amounts of dioritic and granitic rocks. It is up to 10 km thick and exhibits widespread deformation under hypersolidus conditions. The structures indicate emplacement and flow of crystal mush in a dynamic, and possibly extensional, tectonic environment (QUICK et al. 1992). Peak metamorphic conditions of the crustal rocks reached amphibolite (730 ± 50 °C at 0.55 ± 0.10 GPa) and granulite facies conditions (850 ± 100 °C at 0.85 ± 0.05 GPa) in the time span between 296 and 273 Ma (VAVRA et al. 1996, HENK et al. 1997). The sequence is interpreted to represent the intrusion of underplating mantle melts near to the interface between the continental crust and mantle during Permian time (QUICK et al. 1992).

5.2.2. Extension of the event to the east and north

The extension of the Permo-Triassic event to the east and to the north is traced by Permian quartzporphyries and granites. Data of metamorphic rocks are scarce.
Based on the sedimentary record the Transdanubian Central Range Unit (Hungary; part of the Pelso Superunit) has been located between the Austroalpine and Southalpine (Fig. 12) (HAAS et al. 1994). Permian S-type and A-type granites occur in the deepest structural levels at the southern margin of the unit (BUDA et al. 1999).
The palaeogeographic position of the Tisza Superunit is still under discussion. Most authors (HAAS et al. 1994) argue for a localisation west of the ALCAPA terrane (Alpine – Carpathian – Pannonian region), whereas in the reconstruction of STAMPFLI et al. (1999), the Tisza Superunit is adjacent to the western part of the Austroalpine and Southalpine unit. Lower Permian metarhyolites are common in the cover series of the Tisza Superunit on top of a Variscan metamorphic basement (FAZEKAS et al. 1987). In the southeastern

part (Bèkès-Kodru structural unit) similar lithologies as in the Austroalpine Saualpe-Koralpe Complex are known from a basement high below the Tertiary sediments. Biotite-rich lithologies contain polyphase garnets with Permian cores (273 ± 7 Ma) and fine-grained kyanite pseudomorphs after andalusite (LELKES-FELVÀRI et al. 2001).
In the Penninic Tasna Nappe foliated Permian gabbros occur. They are interpreted as lower to middle crustal intrusions (FROITZHEIM & RUBATTO 1998). Lower Permian (c. 270 Ma) S-type and A-type granites are documented from the Gemeric Unit in the Western Carpathians (Slovakia) (FINGER & BROSKA 1999), the Helvetic massifs of the Western Alps (DESMONS et al.1999b) and the Tauern Window in the Eastern Alps (VON QUADT et al. 1999). An extensional regime is likely, but at present no consistent interpretation regarding the Permo-Triassic thermal history of these units exists.

5.3. Thermal evolution and geotectonic setting

In the Austroalpine and Southalpine realm the Permo-Triassic event shows obvious similarities with respect to the observed magmatic rocks, the timing of magmatism and metamorphism, the P-T conditions and the metamorphic assemblages. Further, in both units an extensional environment can be recognised. These facts indicate that the same geodynamic processes are responsible for the Permo-Triassic event in the whole area. The processes were acting more or less simultaneously and were affecting the whole crustal sequences. The available data allow to determine a generalised P-T-t path for the Variscan to Permo-Triassic metamorphic history and give indications for the geotectonic environment.

5.3.1. P-T-t evolution

Typical Variscan metamorphic areas e.g. the northern Ötztal Complex, reached peak metamorphic temperatures at about 340 Ma at a geothermal field gradient of approximately 25 °C/km (DIELLA et al. 1992, TROPPER & HOINKES 1996, THÖNI 1999) (Fig. 10). Subsequent exhumation of the rock pile rose the isotherms condensing them closer to the surface and produced an elevated geothermal field gradient. According to DIELLA et al. (1992) and TROPPER & HOINKES (1996) the value for the geothermal field gradient on the retrograde part of the Variscan P-T path is about 35°C/km. This is a common value, established by exhumation of thickened crust (ENGLAND & HOUSEMAN 1984). At about 310 Ma and 295 Ma the rocks forming the surface for the middle Permian transgressive sediments, cooled down below the closure temperatures of the K-Ar isotopic system in muscovite and the Rb-Sr isotopic system in biotite respectively (THÖNI 1999). Some time later the rocks reached the surface and were partly eroded. Average cooling rates of such exhumation processes are c. 20 °C/Ma (Fig. 11A).
Parts of the Permo-Triassic metamorphic rocks also experienced the first part of this P-T-t path. However, they stayed within the crust and after 290 Ma they underwent decompression and following heating. These processes caused a HT/LP imprint at a geothermal field gradient of about 45 °C/km (Fig. 11B). Metamorphic peak conditions were reached at about 270 Ma. Subsequently the rock pile was

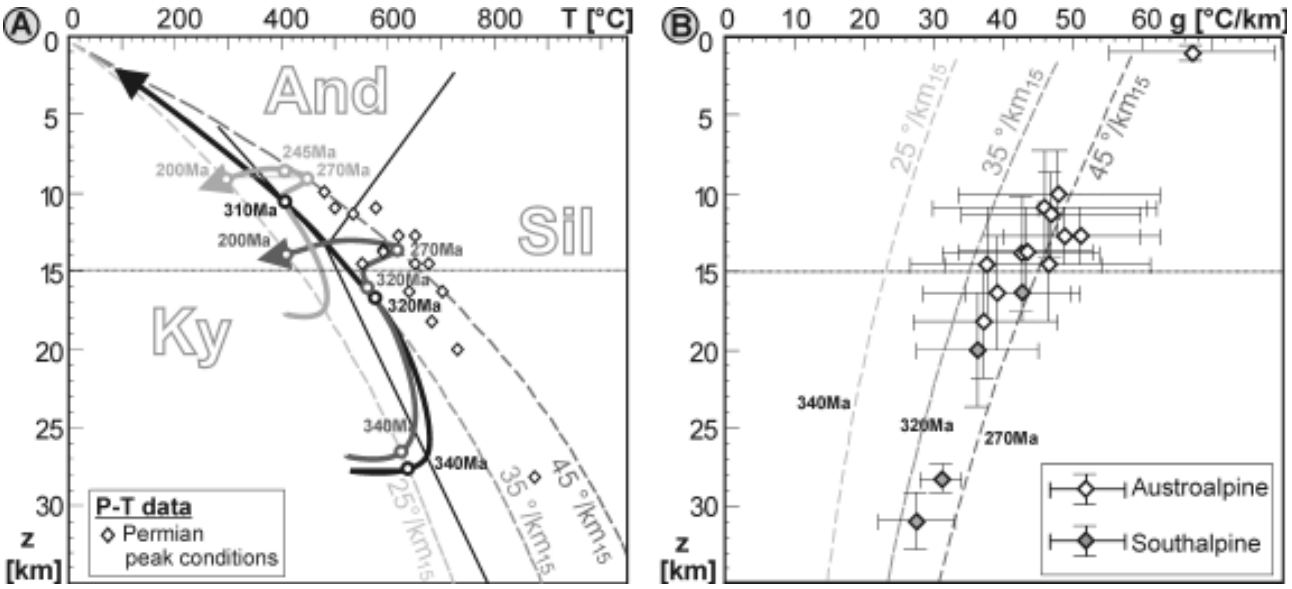

Fig. 10: Interpretation of P-T and geochronological age data from the Austroalpine-Southalpine realm. In both diagrams the geotherms for geothermal field gradients of 25, 35 and 45 °C/km (at 15 km depth) are shown. They correspond to different events in the P-T-t path of the rocks (340 Ma Variscan peak temperature, 320 Ma Variscan exhumation, 270 Ma Permian peak metamorphic conditions. A) P-T-t path for Variscan and Permo-Triassic metamorphic units. The black arrow represents exhumation of Variscan metamorphic rocks. The dark gray and the gray arrow show the P-T-t paths for amphibolite and greenschist metamorphic Permo-Triassic rocks respectively. P-T data shown in the diagrams refer to Table 5. B) geothermal gradient (g) vs. depth (z) values of Permo-Triassic metamorphic units. The geothermal field gradients define a geotherm with c. 45 °C/km at 15 km depth.

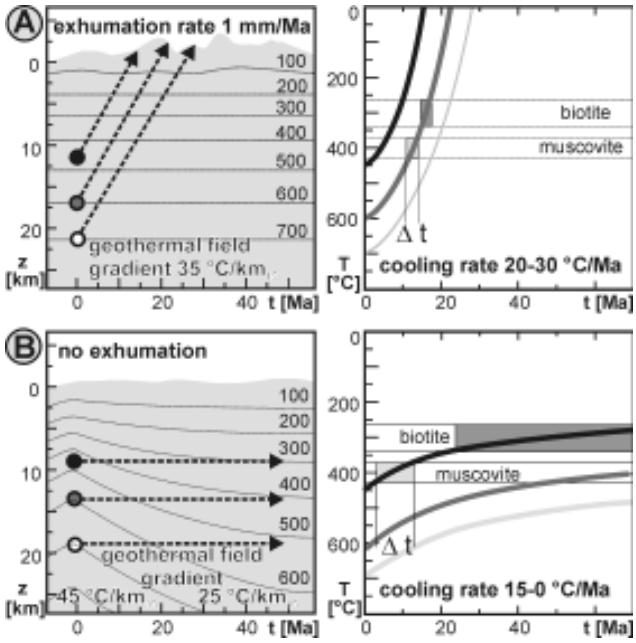

Fig. 11: Comparison of the cooling history in different geotectonic environments. Shown are the blocking temperature ranges of the Ar-Ar and Rb-Sr isotopic systems in biotite and the Ar-Ar isotopic system in muscovite A) During exhumation of thickened crust the cooling rate is increasing with time. The minerals pass through the range of the blocking temperatures within a short time span. B) Cooling in a constant crustal depth by thermal relaxation is characterised by decreasing cooling rates. Minerals remain within the range of their blocking temperature for a long time. Surprisingly Ar-Ar muscovite ages yield similar ages in most of the units south of the SAM. The Rb-Sr and Ar-Ar biotite ages scatter due to grain size effects, fluid activity and excess-Ar respectively.

not exhumed to the surface, but cooled down to the steady state geotherm (c. 25 °C/km), induced by relaxation of the isotherms. Cooling was more or less isobaric, but sedimentation of the Permo-Triassic sedimentary piles and ongoing (maybe localised) extension would have influenced the P-T-t path. However, lower greenschist metamorphic rocks cooled down to below the 400 - 300 °C temperature range at about 270 Ma, whereas andalusite and sillimanite-bearing amphibolite facies rocks passed these temperatures at c. 205 Ma and 190 Ma respectively (see also BERTOTTI et al. 1999). Cooling rates were about 15 °C/Ma at the beginning of the process and were decreasing in the following 70 Ma (Fig. 11B).

5.3.2. Geotectonic setting

HT/LP metamorphism can be caused by (1) exhumation of thickened crust (ENGLAND & HOUSEMAN 1984), (2) contact metamorphism (BARTON & HANSON 1989, STÜWE & POWELL 1989) or (3) lithospheric thinning, especially thinning of the lithospheric mantle (ENGLAND & HOUSEMAN 1984, HARLEY 1989).

In the first case high exhumation rates should have been sustained in the Austroalpine-Southalpine realm until late Permian time. This is not in agreement with the observed extensional regime (e.g. BERTOTTI et al. 1993), the record of marine transgressions and the fine-grained clastic, evaporitic and carbonatic sedimentation at this time (e.g. TOLLMANN 1977, 1985, BERTOTTI et al. 1993). The far extension of the Permo-Triassic thermal event, the homogeneous geothermal field gradient and the volumetrically insignificant amount of plutonic rocks argue against contact metamorphism.
Thinning of the lithosphere is due to extension and causes melting in the lithospheric mantle. If these melts reach the crust mantle boundary magmatic underplating, anatectic melting in the crust and a contemporaneous HT/LP metamorphic imprint will be the result. This scenario describes the observed features of the Permo-Triassic metamorphic event. In fact, the Permian phase in the Alpine realm has already been interpreted as due to underplating of the lower crust by extensive gabbroic intrusions and associated (failed) rifting in the Permian (QUICK et al. 1992, BENCIOLINI 1994, THÖNI 1999).

5.3.3. Sedimentary cover

Basement units with the observed thermal characteristics show subsidence over a long time period. During extension subsidence is induced by the isostatic relaxation of the area. Subsequent cooling of the lithosphere to the relaxed geotherm will lead to a rise in density and thickening of the lithosphere. The result is thermal subsidence.
In the Southalpine realm Permo-Triassic sedimentary piles up to 4 km in thickness (BERTOTTI et al. 1993) are in contact with their basement. Also in the Austroalpine domain the Permo-Triassic sedimentary piles are more than 3 km in thickness. In some places their transgressive contacts to the upper and middle crustal basement is preserved, e.g. Drauzug-Goldeck-Kreuzeck or Silvretta area. The huge masses of the Northern Calcareous Alps are partly overlying low-grade metamorphic rocks of the Greywacke Zone but the middle crustal basement below is truncated. Based on the observed characteristics parts of the Permo-Triassic medium to high-grade metamorphic crystalline units will have been the missing middle crustal basement of the Northern Calcareous Alps.

5.4. Plate tectonic environment and palaeogeographic framework

The Permo-Triassic event is a result of plate tectonic processes. However, it has to be considered that the plate tectonic interpretation is depending on the used palinspastic model. The following discussion is based on the Triassic palinspastic map of HAAS et al. (1995) and the reconstructions of STAMPFLI (1996) and STAMPFLI & MOSAR (1999).
Plotting all areas with indications of a Permo-Triassic extensional event in the Early Permian palaeogeographic map (STAMPFLI 1996) (Fig. 12) they form an east-west orientated zone. To the north a belt of medium- to high-grade

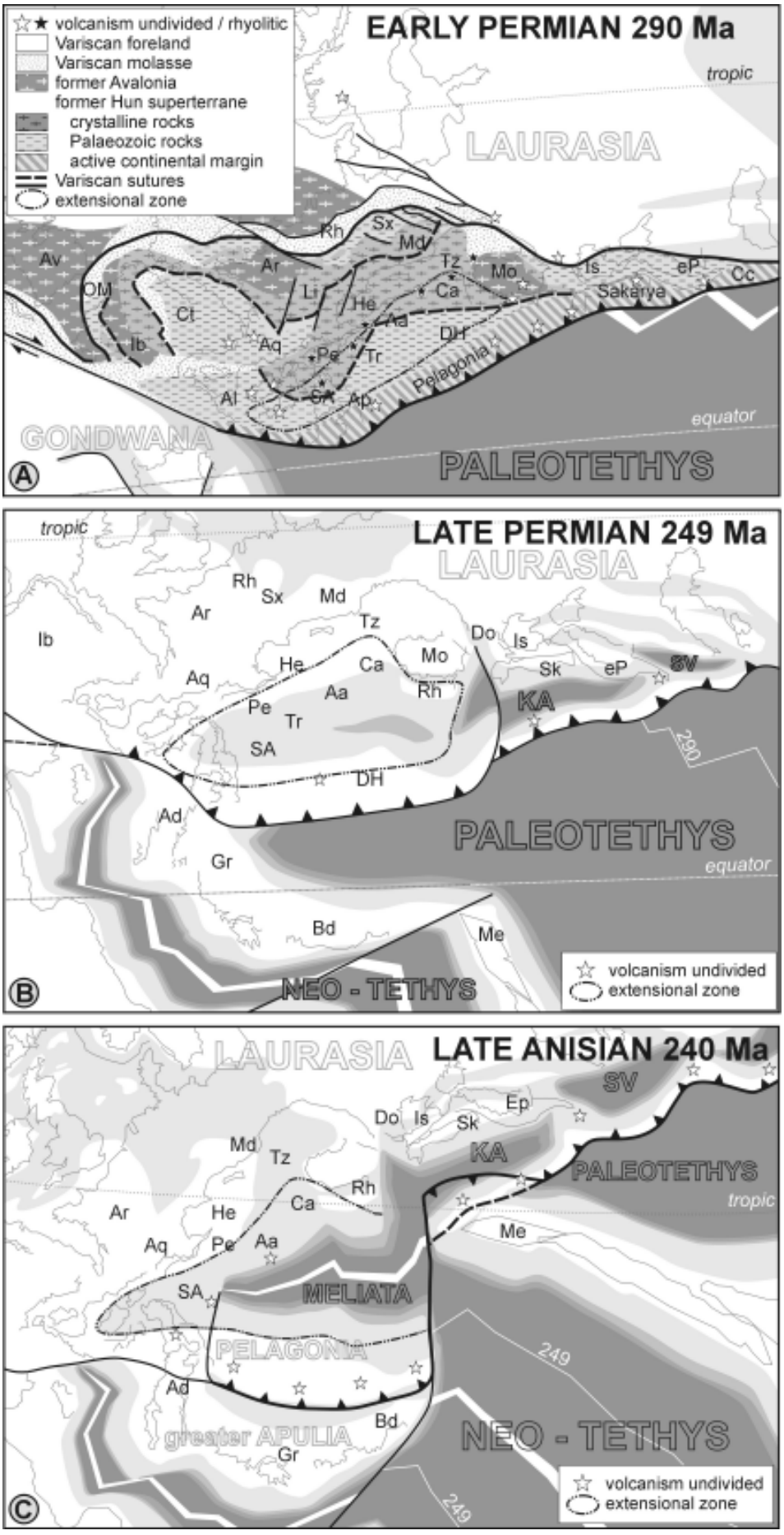

Fig. 12: Paleogeographic framework for the Permo-Triassic event based on the palinspastic reconstructions of STAMPFLI (1996), STAMPFLI & MOSAR (1998) and HAAS et al. (1995).
A) Reconstruction for the Perm-Carboniferous boundary at 290 Ma. The extensional zone is located at the southeastern margin of the Variscan orogene.
B) Extension in late Permian time at c. 250 Ma. caused the formation of an area with thinned continental crust. Marine ingressions led to the deposition of evaporitic sediments and bituminous carbonates in a restricted basin.
C) Ongoing extension causes rifting and the opening of the Meliata Ocean.
A…Austroalpine,
Ad…Adria,
Al…Algeria,
Aq…Aquitania,
A...Avalonia,
Bd…Beydaghlari,
Ca… Carpathians,
Cc…Caucasus,
Ct…Cantabria,
Do…Dobrogea,
DH…Dinarides and Hellenides,
eP…east Pontides,
Gr…Greece,
He…Helveticum,
IA…Inneralpine,
Ib…Iberia,
Is…Istanbul,
KA…Karakaya,
Li…Ligerian,
Md…Moldanubicum,
Me…Menderes,
Mo…Moesia,
OM…Ossa Morena,
Pe…Pennine,
Rh…Rhenohercynicum,
Ro…Rhodope,
SA…Southalpine,
Sk…Sakarya,
SV…Svanetia,
Sx…Saxothuringicum,
Tr…Transdanubia,
Tz…Tisza.

metamorphic rocks, exhumed to the surface during the Variscan orogeny (e.g. Aquitaine Massif, Helvetic Zone, Moldanubic Zone) is located. The southern margin was probably formed by parts of Adria, the Hellenides and Dinarides.

The Austroalpine and Southalpine have been part of the Hun superterrane which separated from the northern margin of Gondwana in Early Paleozoic times (c. 435 Ma). During the Variscan collisional event (380 - 300 Ma) this superterrane was squeezed between former accreted Baltica, Laurentia and Avalonia in the north and the Gondwana continent in the south. According to STAMPFLI (1996) the southeastern border of the Variscan orogen was an active continental margin below which the westernmost part of the Palaeotethyan ocean was subducted (Fig. 12A). In Permian time (290 – 249 Ma) the Paleotethys mid-ocean ridge was moving eastward and slab roll back of the western Paleotethys induced extension on the southern margin of Laurasia. In the Variscan foreland in the east, small oceanic back arc basins were formed (Fig. 12B). More to the west, extension affected the southern part of the Variscan orogen, which was highly ductile due to the increased geothermal gradient (c. 35 °C/km). However, the extension of the Palaeotethys to the west and the proposed subduction zone is not well constrained yet. On the other hand palaeomagnetic data indicate a clockwise rotation of Adria and Gondwana with respect to the Variscan consolidated part of Europe during Permian time (MAURITSCH 1992). Alternatively this rotation could have caused stretching within the extensional zone.

Stretching resulted in thinning of the lithosphere, magmatic underplating and a HT/LP metamorphic event with a geothermal gradient of more than 45° C/km in Permian time. Isostatic relaxation of the area caused the formation of a non-oceanic basin separated from the Paleotethys ocean. Restricted water exchange with the ocean was responsible for the sedimentation of evaporites and bituminous carbonates. Ongoing extension within the thinned and cooling crust caused rifting and opening of the Meliata ocean in late Anisian time (240 Ma) (Fig. 12C). This process is accompanied by the magmatic pulse in Anisian and Ladinian time. The opening of this oceanic realm was responsible for a first cycle of facies differentiation in the Austroalpine-Southalpine realm.

Acknowledgements

The authors thank M. Jelenc and M. Thöni for their help with the Rb-Sr and Sm-Nd isotope analyses; K. Schuster, Ch. Miller, K. Stüwe, F. Neubauer and D. Robinson for their critical review of the manuscript. This work has been supported by the *Fonds zur Förderung der wissenschaftlichen Forschung* (Project No. S47-GEO and P12277-GEO).

References

AMMAN, A. (1985): Zur Metamorphose des nördlichen Silvrettakristallins. - Unpubl. Diss. Naturwiss. Fak Univ. Innsbruck, 1-114, Innsbruck.

BARTH, S., OBERLI, F. & MEIER, M. (1994): Th-Pb versus U-Pb isotope systematics in allanite from co-genetic rhyolite and granodiorite: implications for geochronology. - Earth Plan. Sci. Lett., **124**: 149-159, Amsterdam.

BARTON, M.D. & HANSON, R.B. (1989): Magmatism and the development of low pressure metamorphic belts: Implications from the western United States and thermal modelling. - GSA Bulletin, **101**: 1051-1065, Boulder.

BECK-MANNAGETTA, P. (1970): Über den geologischen Aufbau der Koralpe. - Verh. Geol. B.-A., **1970**: 491-496, Wien.

BENCIOLINI, L. (1994): Metamorphic evolution of the Silvretta gabbro and related rocks (Upper Austroalpine, Central Alps). Its bearing on the pre-Mesozoic history of the alpine area basement. - Mem. Sci. Geol., **46**: 353-371, Padova.

BERMAN, R.G. (1988): Internally-consistent thermodynamic data for minerals in the system Na2O - K2O – CaO – MgO – FeO - Fe2O3 - Al2O3 - SiO2 - TiO2 -H2O - CO2. - J. Petrol., **29/2**: 445-522, Oxford.

BERNHARD, F., SCHITTER, F. & FINGER, F. (1998): Zur Altersstellung der Lazulith Quarz-Gänge im unterostalpinen Grobgneiskomplex der Nordoststeiermark und des südlichen Niederösterreich. - Mitt. naturwiss. Vereins Stmk, **128**: 43-56, Graz.

BERNHARD, F., FINGER, F. & SCHITTER, F. (2000): Timing of metamorphic, magmatic, hydrothermal and deformational events revealed by EMP total Pb dating of monazite and xenotime in the polymetamorphic Austroalpine Grobgneis complex, Eastern Alps, Styria, Austria. - Abstracts Vol. 31st Internat. Geol. Congress, Rio de Janeiro, Brazil. Session 18-3, Rio de Janeiro.

BERKA, R. (2000): Die Stellung der Traibachschiefer im Semmering-Wechsel System. - Unpub. Diploma Thesis Formal-Natwiss. Fak. Univ. Wien, 1-133, Wien.

BERTOTTI, G., PICOTTI, V., BERNOULLI, D. & CASTELLARIN, A. (1993): From rifting to drifting: tectonic evolution of the South-Alpine upper crust from the Triassic to the Early Cretaceous. - Sedimentary Geology, **86**: 53-76, Amsterdam.

BERTOTTI, G., SEWARD, D., WIJBRANS, J., TER VOORDE, M. & HURFORD, A.J. (1999): Crustal thermal regime prior to, during, and after rifting: A geochronological and modelling study of the Mesozoic South Alpine rifted margin. - Tectonics, **18/2**: 185-200, Washington.

BOCKEMÜHL, C. (1988): Der Marteller Granit (Südtirol Italien). - PhD Thesis Phil.- Naturwiss. Fak. Univ. Basel, 1-143, Basel.

BOLE, M., DOLENEC, T., ZUPANCIC, N. & CINIC-JUHANT, B. (2001): The Karavanke Granitic Belt (Slovenia) - a bimodal Triassic alkaline plutonic complex. - Schweiz. Mineral. Petrogr. Mitt., **81**: 23-38, Zürich.

BONIN, B., BRÄNDLEIN, P., BUSSY, F., DESMONS, J., EGGENBERGER, U., FINGER, F., GRAF, K., MARPO, CH., MERCOLLI, I., OBERHÄNSLI, R., PLOQUIN, A., VON QUADT, A., VON RAUMER, J., SCHALTEGGER, U., STEYRER, H.P., VISONÀ, D. & VIVIER, G. (1993): Late Variscan Magmatic Evolution of the Alpine Basement. - (In: NEUBAUER, F. & VON RAUMER, J.F. (Eds.): The pre- Mesozoic Geology of the Alps), 172-201, Springer, Berlin-Heidelberg-New York.

BORIANI, A. & BURLINI, L. (1995): Carta geologica della Valle Cannobina. Scala 1:25000. - Comunità Montana Valle Cannobina, Dipartimento di Scienza della Terra dell' Università degli Studi di Milano, Centro di Studio per la Geodinamica Alpina e Quarternaria del CNR-Milano. Grafiche Diodoro, Milano.

BORSI, S., DEL MORO, A & FERRARA, G. (1972): Età radiometriche delle rocce intrusive del massiccio di Bressanone-Ivigna-Monte Croce (Alto Adige). - Bollettino della Società Geologica Italiana, **91/2**: 387-406, Roma.

BORSI, S., DEL MORO, A., SASSI, F.P., VISONA, D. & ZIRPOLI, G. (1980): On the existence of Hercynian aplites and pegmatites in the lower Aurina valley (Ahrntal, Austrides, Eastern Alps). - N.

Jb. Miner. Mh., **1980/11**: 501-514, Stuttgart.

BORSI, S., FERRARA, G., PAGGANELLI, L. & SIMBOLI, G. (1968): Isotopic age measurements of the M. Monzoni intrusive Complex. - Miner. Petrogr. Acta, **14**: 171-183.

BREWER, M.S. (1970): K-Ar Age Studies in the Eastern Alps: the Oberostalpindecke of Kärnten. - Phil. Diss. Univ. Oxford: 1-213, Oxford.

BRODIE, K.H., REX, D. & RUTTER, E.H. (1989): On the age of deep crustal extensional faulting in the Ivrea zone, northern Italy. - (In: COWARD. M.P. et al. (Eds.): Alpine tectonics. - Geol. Soc. London Special Publications, **45**: 203-210, London.

BUDA, G., LOVAS, G., KLÖTZLI, U. & COUSENS, B.L. (1999): Variscan granitoids of the Mòràgy Hills (Southern Hungary). - Berichte der Deutschen Mineralogischen Gesellschaft, Beih. z. Eur. J. Mineral., **11/2**: 21-34, Stuttgart.

BURGHELE, A. (1987): Propagation of error and choice of standard in the 40Ar/39Ar technique. - Chem. Geol., **66**: 17-19, Amsterdam.

BÜRGI, A. & KLÖTZLI, U. (1987): New Data on the Evolutionary History of the Ivrea Zone (Northern Italy). - Bull. Swiss Assoc. Petrol. Geologists and -Engineers, **56/130**: 49-70, Zürich.

CASTELLARIN, A., LUCCHINI, F., ROSSI, L.P., SELLI, L. & SIMBOLI, G. (1988): The middle Triassic magmatic-tectonic arc development in the Southern Alps. - Tectonophysics, **146**: 79-89, Amsterdam.

CLIFF, R.A., HOLZER, H.F. & REX, D.C. (1974): The age of the Eisenkappel Granite, Carinthia and the History of the Periadriatic Lineament. - Verh. Geol. B.-A., **2-3**: 347-350, Wien.

COLOMBO, A. & TUNESI, A. (1999): Pre-Alpine metamorphism of the Southern Alps west of the Giudicarie Line. - Schweiz. Mineral. Petrogr. Mitt., **79**: 63-77, Zürich.

DALLMEYER, R. D., HANDLER, R., NEUBAUER, F. & FRITZ, H. (1998): Sequence of thrusting within a thick-skinned tectonic wedge: evidence from 40Ar/39Ar and Rb-Sr ages from the Austroalpine nappe complex of the Eastern Alps. - J. Geol., **106**: 71-86, Chicago.

DALRYMPLE, G. B., ALEXANDER, E. C. LANPHERE, M.A. & KRAKER, G.P. (1984): Irradiation of samples for 40Ar/39Ar dating using the Geological Survey TRIGA reactor. U. S. Geological Survey Professional Papers, **1176**: 1-55, U.S. Geological Survey, Reston.

DEL MORO, A., NOTARPIETRO, A. & POTENZA, R. (1981): Revisione del significato strutturale delle masse intrusive minori dellàlta Valtellina: risultati priliminari. - Rend. Soc. It. Miner. Petr., **38(1)**: 89-96, Pavia.

DESMONS, J., COMPAGNONI, R. & CORTESOGNO, L. with the collaboration OF FREY, M., GAGGERO, L., DALLAGIOVANNA, G., SENO, S. AND RADELLI, L. (1999b): Alpine metamorphism of the Western Alps: II. High-P/T and related pre-greenschist metamorphism. - Schweiz. Mineral. Petrogr. Mitt., **79/1**: 111-134, Zürich.

DESMONS, J., COMPAGNONI, R., CORTESOGNO, L., FREY, M. & GAGGERO, L. (1999a): Pre-Alpine metamorphism of the Internal zones of the Western Alps. - Schweiz. Mineral. Petrogr. Mitt., **79/1**: 23-39, Zürich.

DIELLA, V., SPALLA, M.I. & TUNESI, A. (1992): Contrasting thermomechanical evolutions in the Southalpine metamorphic basement of the Orobic Alps (Central Alps, Italy). - J. metamorphic Geol., **10**: 203-219, Oxford.

DI PAOLA, S. & SPALLA, M.I. (2000): Contrasting tectonic records in the pre-Alpine metabasites of the Southern Alps (Lake Como, Italy).- J. Geodynamics, Oxford, (in press).

DRAGANITS, E. (1998). Seriengliederung im Kristallin des südlichen Ödenburger Gebirges (Burgenland) und deren Stellung zum Unterostalpin am Alpenostrand. - Jb. Geol. B.-A., **141**: 113-146, Wien.

ENGLAND, P. & HOUSEMAN, A.B. (1984): Pressure-Temperature-Time Paths of Regional Metamorphism I. Heat Transfer during the Evolution of Regions of Thickenend Continental Crust. - J. Petrol., **25/4**: 894-928, Oxford.

EXNER, CH. (1972): Geologie der Karawankenplutone östlich von Eisenkappel (Kärnten). - Mitt. Österr. Geol. Ges., **64**: 1-108, Wien.

FAZEKAS, V., MAJOROS, G. & SZEDERKÉNYI, T. (1987): Lower Permian volcanic sequences of Hungary. - Acta Geol. Hung., **30/1-2**: 21-34, Budapest.

FERRARA, G. & INNOCENTI, F. (1974): Radiometric age evidence of a Triassic thermal event in the Southern Alps. - Geol. Rdschau, **63**: 572-581, Stuttgart.

FERREIRO MÄHLMANN, R. & PETSCHICK, R. (1996): The coalification map of the Alps between the rivers Inn, Isar and Rhein (Austria, Switzerland). - Mitt. Österr. Miner. Ges., **141,** 85-86, Wien.

FINGER, F. & BROSKA, I. (1999): The Gemeric S-type granites in southeastern Slovakia: Late Palaeozoic or Alpine intrusions? Evidence from electron-microprobe dating of monazite. - Schweiz. Mineral. Petrogr. Mitt., **79**: 439-443, Zürich.

FLISCH, M. (1986): Die Hebungsgeschichte der oberostalpinen Silvretta-Decke seit der mittleren Kreide. - Bull. Ver. schweiz. Petroleum-Geol. u. Ing., **53/123**: 23-49, Zürich.

FRANK, W., ESTERLUS, E., FREY, I., JUNG, G., KROHE, A. & WEBER, J. (1983): Die Entwicklungsgeschichte von Stub- und Koralmkristallin und die Beziehung zum Grazer Paläozoikum. - Jber. 1982 Hochschulschwerpkt. S15, **(1982)**: 263-293, Graz.

FROITZHEIM, N. & RUBATTO, D. (1998): Continental breakup by detachment faulting: field evidence and geochronological constrains (Tasna Nappe, Switzerland). - Terra Nova, **10**: 171-176, Oxford.

FROITZHEIM, N., SCHMIDT, S.M. & FREY, M. (1996): Mesozoic paleoegeography and the timing of eclogitefacies metamorphism in the Alps: A working hypothesis. - Eclogae geol. Helv., **89/1**: 81-110, Basel.

GAAL, G. (1966): Geologie des Roßkogelgebietes W Mürzzuschlag (Steiermark). - Mitt. Ges. Geol. Bergbaustud., **16**: 105-148, Wien.

GAZZOLA, D., GOSSO, G., PULCRANO, E. & SPALLA, M.I. (2000): Eo-Alpine HP metamorphism in the Permian intrusives from the steep belt of the central Alps (Languard-Campo nappe and Tonale Series). - Geodynamica Acta, **13**: 149-167.

GENSER, J. & NEUBAUER, F. (1989): Architektur und Kinematik der östlichen Zentralalpen - eine Übersicht. - Mitt. Naturwiss. Ver. Steiermark, **120**: 203-219, Graz.

GRAUERT, B. (1969): Die Entwicklungsgeschichte des Silvretta-Kristallins auf Grund radiometrischer Altersbestimmungen. - Inauguraldiss. Phil.-naturwiss. Fak. Univ. Bern, 1-166, Bern.

GREGNANIN, A. (1980): Metamorphism and magmatism in the western Italian Tyrol. - Rend. Soc. It. Miner. Petr., **36(1)**: 49-64, Pavia.

GREGUREK, D. (1995): Geothermobarometrische Untersuchungen an den Gesteinen der südlichen Koralpe. - Unpub. Diploma Thesis Naturwiss. Fak. Karl-Franzens-Universität Graz, 1-224, Graz.

HAAS, R. (1985): Zur Metamorphose des südlichen Ötztalkristallins unter besonderer Berücksichtigung der Matscher Einheit (Vintschgau/Südtirol). - Unpub. Thesis Naturwiss. Fak. Univ. Innsbruck, 1-118, Innsbruck.

HAAS, J., KOVÀCS, S., KRYSTYN, L. & LEIN, R. (1994): Significance of Late Permian-Triassic facies zones in terrrane reconstructions in the Alpine-North Pannonian domain. - Tectonophysics, **242**: 19-40, Amsterdam.

HABLER, G. & THÖNI, M. (1998): Die prämesozoische Niederdruckmetamorphose in der polymetamorphen Gneisgruppe der NW Saualpe (Arbeitsgebiet N Knappenberg /Kärnten). - Mitt. Österr. Miner. Ges., **143**: 291-293.

HABLER, G. (1999): Die polyphase Metamorphose- und Strukturprägung der Eklogit-führenden ostalpinen Kristallineinheiten im Raum Knappenberg (NW Saualpe, Kärnten). - Unpub. Diploma Thesis Formal- Naturwiss. Fak. Univ. Wien, 1-150, Wien.

HADITSCH, J.G., LEICHTFRIED, W. & MOSTLER, H. (1979): Über ein stratiformes Schwerspatvorkommen in unterpermischen Schich-

ten des Montafons (Vorarlberg). - Geol.-Paläont. Mitt. Innsbruck, **7/6**: 1-14, Innsbruck.

HARLEY, S.L. (1989): The origin of Granulites: a metamorphic perspective. - Geol. Mag., **126**: 215-247, Cambridge University Press, Cambridge.

HEEDE, H.-U. (1997): Isotopengeologische Untersuchungen an Gesteinen des ostalpinen Saualpenkristallins, Kärnten. - Österreich. Münster. Forsch. Geol. Paläont., **81**: 1-168, Münster.

HENK, A., FRANZ, L., TEUFEL, S. & ONCKEN, O. (1997): Magmatic underplating, extension, and crustal reequilibration: insights from a cross-section through the Ivrea Zone and Strona-Ceneri Zone, Northern Italy. - J. Geol., **105**: 367-377, Chicago.

HOERNES, S. (1971): Petrographische Untersuchungen an Paragneisen des polymetamorphen Silvrettakristallins. - Tschermaks Min. Petr. Mitt., **15**: 56-70, Wien.

HOINKES, G., KOLLER, F., HÖCK, V., NEUBAUER, F., RANTITSCH, G. & SCHUSTER, R. (1999): Alpine metamorphism of the Eastern Alps. - Schweiz. Mineral. Petrogr. Mitt., **79**: 155-181, Zürich.

HOISCH, T.D. (1991): Equilibria within the mineral assemblage quartz + muscovite + biotite + garnet + plagioclase, and implications for the mixing properties of octahedrally coordinated cations in muscovite and biotite. - Contrib. Mineral. Petrol., **108**: 43-54: Heidelberg-New York.

HOKE, L. (1990): The Altkristallin of the Kreuzeck Mountains, SE-Tauern Window, Eastern Alps - Basement Crust in a convergent plate Boundary Zone. - Jb. Geol. B.-A., **133**: 5-87, Wien.

JÄGER, E. (1979): Introduction to Geochronology. - (In: JÄGER, E. & HUNZIGER, J.C. (Eds): Lectures in Isotopegeology), 1-12, Springer, Berlin Heidelberg New York.

KRECZY, L. (1981): Seriengliederung, Metamorphose und Altersbestimmung in der Region der Thialspitze SW Landeck, Tirol. – Unpub. Diss. Formal.- Naturwiss. Fak. Univ. Wien, 1-125, Wien.

KÜMEL, F. (1935): Die Sieggrabener Deckscholle im Rosaliengebirge (Niederösterreich-Burgenland). - Miner. Petrogr. Mitt., **47**: 141-184, Wien.

LARDEAUX, J.M. & SPALLA M.I. (1991): From granulites to eclogites in the Sesia zone (Italian Westen Alps): a record of the opening and closure of the Piedmont ocean. - J. metamorphic Geol., **9**: 35-59, Oxford.

LELKES-FELVÁRI, GY., FRANK, W. & SCHUSTER, R. (2001): Basement evolution of the Great Hungarian Plain: Variscan, Permo-Triassic and Alpine (Cretaceous and Tertiary) metamorphism. - PANCARDI 2001, (in press).

LELKES-FELVÀRI, GY. & SASSI, F.P. (1984): Pre-alpine and alpine developments of the austridic basement in the Sopron area (Eastern Alps, Hungary). - Rend. Soc. It. Miner. Pet., **39**: 593-612, Milano.

LICHEM, CH., GREGUREK, D. & HOINKES G. (1996): Alpidische Metmorphosegradienten im Koralmkristallin. 6. Symposium Tektonik – Strukturgeologie – Kristallingeologie, erweiterte Kurzfassungen, 253-254. Facultas-Universitätsverlag, Wien.

LICHEM, CH., HOINKES, G. & GREGUREK, D. (1997): Polymetamorphism of the Austroalpine Koralm basement: New evidence for a Permian event. - Abstract Supplement No.1, Terra Nova, **9**: 489, Oxford.

LIPPOLT, H.T. & PIDGEON, R. (1974): Isotopic Mineral Ages of a Diorite from the Eisenkappel Intrusion, Austria. - Zeitschrift für Naturforschung Wiesbaden, **29a**: 966-968, Wiesbaden.

MANDL, G. & ONDREJICKOVA, A. (1993): Radiolarien und Conodonten aus dem Meliatikum im Ostabschnitt der NKA (A). - Jb. Geol. B.-A., **136/4**: 841-871, Wien.

MARSCH, F.W. (1983): Spodumenkristalle in einem Pegmatit der Kreuzeckgruppe. – Mitt. Österr. Miner. Ges., **129**:13-18, Wien.

MAURITSCH H.J. (1992): Palaeomagnetic Data from the Palaeozoic Basement of the Alps. - (In: NEUBAUER, F. & VON RAUMER, J.F. (Eds.): The pre- Mesozoic Geology of the Alps), 41-51. Springer, Berlin-Heidelberg-New York.

MICHARD, A., GURRIET, P., SOUDANT, M. & ALBAREDE, F. (1985): Nd isotopes in French Phanerozoic shales: external vs. internal aspects of crustal evolution. - Geochim. Cosmochim. Acta, **49**: 601-610, Oxford.

MILLER, CH. & THÖNI, M. (1997): Eo-Alpine eclogitisation of Permian MORB-type gabbros in the Koralpe (Eastern Alps, Austria): new geochronological, geochemical and petrological data. - Chem. Geol., **137**: 283-310, Amsterdam.

MILOTA, CH. (1983): Die Sieggrabener Deckscholle im südlichen Rosaliengebirge (Niederösterreich/ Burgenland). - Unpub. Vorarbeit Inst. Geol. Univ. Wien, 1-92, Wien.

MOINE, B., FORTUNE, J.P., MOREAU, P. & VIGUIER, F. (1989): Comparative mineralogy, geochemistry, and conditions of formation of two metasomatic talc and chlorite deposites: Trimouns (Pyrenees, France) and Rabenwald (Eastern Alps, Austria). - Economic Geology, **84**: 1398-1416, Lancaster.

MORAUF, W. (1980): Die permische Differentiation und die alpidische Metamorphose des Granitgneises von Wolfsberg, Koralpe, SE-Ostalpen, mit Rb/Sr- und K/Ar-Isotopenbestimmungen. - Tschermaks Mineral. Petrogr. Mitt. **27**: 169-185, Wien.

MÜLLER, W., DALLMEYER, D., NEUBAUER, F. & THÖNI, M. (1999): Deformation-induced resetting of Rb/Sr and 40Ar/39Ar mineral systems in a low-grade, polymetamorphic terrane (Eastern Alps, Austria). - J. Geol. Soc. London, **156**: 261-278, London.

NEUBAUER, F., DALLMEYER, R.D. & TAKASU, A. (1999a): Conditions of eclogite formation and age of retrogression within the Sieggraben unit, Eastern Alps: implications for Alpine-Carpathian tectonics. - Schweiz. Mineral. Petrogr. Mitt., **79/2**: 297-307, Zürich.

NEUBAUER, F., HOINKES, G., SASSI, F.P., HANDLER, R., HÖCK, V., KOLLER, F. & FRANK, W. (1999b): Pre-Alpine metamorphism in the Eastern Alps. - Schweiz. Mineral. Petrogr. Mitt., **79**: 41-62, Zürich.

OBENHOLZNER, J.H. (1991): Triassic volcanogenic sediments from the Southern Alps (Italy, Austria, Yugoslavia) - a contribution to the „Pietra verde“ problem. - Sedimentary Geology, **74**: 157-171, Amsterdam.

PHILIPPITSCH, R., MALECKI, G. & HEINZ H. (1986): Andalusit-Granat-Staurolith-Glimmerschiefer im Gailtalkristallin (Kärnten). - Jb. Geol.-B. A., **129/1**: 93-98, Wien.

PIN, C. (1986): Datation U-Pb sur zircons à 285 M.a. du complex gabbro-diorique du Val Sesia - Val Mastallone et àge tardihercynien du mètamorphisme granulitique de la zone Ivrea-Verbano (Italie). - C.R. Acad. Sc. Paris, **303 (II)**:827-829, Paris.

PLYUSNINA, L.P. (1982): Geothermometry and Geobarometry of Plagioclase-Hornblende Bearing Assemblages. - Contrib. Mineral. Petrol., **80**, 10-146, Heidelberg-New York.

PUMHÖSL, H., KOLLER, F., EL DALOK, A., SEIFERT-FALKNER, C., THÖNI, M. & FRANK, W. (1999): Origin and evolution of gabbroic intrusions within the Grobgneis-Unit, Lower Austroalpine Unit (Eastern Alps). - Berichte der Deutschen Mineralogischen Gesellschaft, Beih. z. Europ. J. Mineral., **11**: 185, Stuttgart.

PUMHÖSL, H., KOLLER, F., FARYAD, S.W., SEIFERT-FALKNER, C., FRANK, W., MILLER, C. & SATIR, M. (submitted): Origin and evolution of Permian gabbroic intrusions within the Lower Austroalpine Grobgneiss Unit (Eastern Alps). - Chem. Geol., Amsterdam.

PUTIS, M., KORIKOVSKY, S.P. & PUSHKAREV, Y.D. (2000): Petrotectonics of an Austroalpine Eclogite-Bearing Complex (Sieggraben, Eastern Alps) and U-Pb Dating of Exhumation. - Jb. Geol. B.-A., **142**: 73-93, Wien.

VON QUADT, A., HAUNSCHMID, B. & FINGER, F. (1999): Mid-Permian A-Type plutonism in the eastern Tauern-Window. - Berichte der Deutschen Mineralogischen Gesellschaft, Beih. z. Europ. J. Mineral., **11**: 185, Stuttgart.

QUICK, J., SINIGOI, S., NEGRINI, L., DEMARCHI, G. & MAYER, A.

(1992): Synmagmatic deformation in the underplated igenous complex of the Ivrea-Verbano zone. - Geology, **20**: 613-616, Boulder.

RATSCHBACHER, L. (1986): Kinematics of Austro-Alpine cover nappes: changing translation path due to transpression. - Tectonophysics, **125**: 335-356, Amsterdam.

ROCKENSCHAUB, M., KOLENPRAT, B. & FRANK, W. (1999): The tectonometamorphic evolution of Austroalpine Units in the Brenner Area (Tirol, Austria) New geochronological implications. - Tübinger Geowissenschaftliche Arbeiten, Serie A, **52**: 118-119, Tübingen.

ROTTURA, A., DEL MORO, A., CAGGIANELLI, A., BARGOSSI, G.M. & GASPAROTTO, G. (1997): Petrogenesis of the Monte Croce granitoids in the context of Permian magmatism in the Southern Alps, Italy. - Eur. J. Mineral., **9**: 1293-1310, Stuttgart.

SAMSON, S.D. & ALEXANDER, E.C. (1987): Calibration of the interlaboratory 40Ar/39Ar dating standard, Mmhb-1. - Chemical Geology, **66**: 27-34, Amsterdam.

SANDERS, C.A.E., BERTOTTI, G., TOMASINI, S., DAVIS, G.R. & WIJBRANS, J.R. (1996): Triassic pegmatites in the Mesozoic middle crust of the Southern Alps (Italy): Fluid inclusions, radiometric dating and tectonic implications. - Eclogae geol. Helv., **89/1**: 505-525, Basel.

SATIR, M. (1975): Die Entwicklungsgeschichte der westlichen Hohen Tauern und der südlichen Ötztalmasse auf Grund radiometrischer Altersbestimmungen. - Mem. Ist. Geol. Miner. Univ. Padova, **30**: 82, Padova.

SCHALTEGGER, U. & BRACK, P. (1999): Short-Lived Events of Extension and Volcanism in the Lower Permian of the Southern Alps (Northern Italy, Southern Switzerland). - EUG10 Strasbourg, J. Conf. Abs. **4/1**: 296-297, Cambridge.

SCHARBERT, S. (1975): Radiometrische Altersdaten von Intrusivgesteinen im Raum Eisenkappel (Karawanken, Kärnten). – Verh. Geol. B.-A., **1975/4**: 301-304, Wien.

SCHARBERT, S. (1990): Rb-Sr Daten aus dem Raabalpenkristallin. (In: PEINDL, P., NEUBAUER, F. MOYSCHEWITZ, G., REINDL, H. & WALLBRECHER, E. (Eds.): Die geologische Entwicklung des südlichen Raabalpen- und Wechselkristallins, Excursion guide TSK III Excursion „Raabalpen- und Wechselkristallin"), 22-25. - Geologisches Institut der Universität Graz, Graz.

SCHMIDT, R. & WOOD, B.J. (1976): Phase relationships in granulitic metapelites from the Ivrea-Verbano zone (Northern Italy). - Contrib. Mineral. Petrol., **54**: 255-279, Heidelberg-New York.

SCHULZ, B., SIEGESMUND, S., STEENKEN, A., SCHÖNHOFER, R. & HEINRICHS, T. (2001): Geologie des ostalpinen Kristallins südlich des Tauernfensters zwischen Virgental und Pustertal. - Z. dt. geol. Ges., **152** (in print).

SCHUSTER, K., BERKA, R., DRAGANITS, E., FRANK, W. & SCHUSTER, R. (2001a): Lithologien, Metamorphosegeschichte und tektonischer Bau der kristallinen Einheiten am Alpenostrand. - Arbeitstagung Geol. B.-A. 2001 - Neuberg an der Mürz, 29-56 Wien

SCHUSTER, R. & FAUPL, P. (2001): Permo-Triassic sedimentary record and contemporaneous thermal basement evolution in the Drauzug-Goldeck-Kreuzeck area (Eastern Alps/Austria). - Geol. Paläont. Mitt. Innsbruck, **25**: 192-194, Innsbruck.

SCHUSTER, R. & FRANK, W. (2000): Metamorphic evolution of the Austroalpine units east of the Tauern Window: indications for Jurassic strike slip tectonics. - Mitt. Ges. Geol. Bergbaustud. Österreich, **42** (1999**):** 37-58, Wien.

SCHUSTER, R., PROYER, A., HOINKES, G. & SCHULZ, B. (2001b): Indications for a Permo-Triassic metamorphic imprint in the Austroalpine crystalline rocks of the Defereggen Alps (Eastern Tyrol). - Mitt. Österr. Miner. Ges., **146**: 275-277 Wien.

SCHUSTER, R. & SCHUSTER, K. (2001): Permo-Triassic ductile deformation in the Austroalpine Strieden Complex (Kreuzeck Mountains / Austria). - Geol. Paläont. Mitt. Innsbruck, **25**: 197-198, Innsbruck..

SCHUSTER, R. & THÖNI, M. (1996): Permian Garnet: Indications for a regional Permian metamorphism in the southern part of the Austroalpine basement units. - Mitt. Österr. Miner. Ges., **141**: 219-221, Wien.

SENARCLENS-GRANCY, W. (1972): Geologische Karte der westlichen Deferegger Alpen 1:25 000. - Geol. B.-A. Österreich, Wien.

SILLETTO, G.B., SPALLA, M.I., TUNESI, A., LARDEAUX, J.M. & COLOMBO, A. (1993): Pre-Alpine structural and metamorphic histories in the Orobic Southern Alps, Italy. - (In:) NEUBAUER, F. & VON RAUMER, J.F. (Eds.): Pre-Alpine basement in the Alps, 583-596, Springer Verlag (Heidelberg).

SILLS, J.D. (1984): Granulite facies metamorphism in the Ivrea zone, N.W. Italy. - Schweiz. Mineral. Petrogr. Mitt., **64**: 169-191, Zürich.

SPEAR, F.S. (1993): Metamorphic Phase Equilibria and Pressure-Temperature-Time Paths. - Mineralogical Society of America Monograph, 799pp, (Washington).

SPIESS, R. (1987): The Early Alpine overprint in the northern Silvrettakristallin and the western "Phyllitgneiszone" (Vorarlberg-Tirol, Austria): radiometric evidence. - Rend. Soc. It. Miner. Pet., **42**: 193-202, Milano.

SPIESS, R. (1995): The Passeier-Jaufen Line: a tectonic boundary between Variscan and eo-Alpine Merane Mauls basement. - Schweiz. Mineral. Petrogr. Mitt., **75:** 413-425, Zürich.

STÄHLE, V., FRENZEL, G., HESS, J.C., SAUPE, F., SCHMIDT, S.TH. & SCHNEIDER, W. (2001): Permian metabasalt and Triassic alkaline dykes in the northern Ivrea zone:clues to the post-Variscan geodynamic evolution of the Southern Alps. - Schweiz. Mineral. Petrogr. Mitt., **81**: 1-21, Basel.

STAMPFLI, G.M. (1996): The Intra-Alpine terrain: a Paleotethyan remnant in the Alpine Variscides. - Eclogae geol. Helv., **89**: 13-42, Basel.

STAMPFLI, G.M. & MOSAR, J. (1999): The making and becoming of Apulia. - Memorie di Scienze Gelogiche, **51/1**: 141-154, Padova.

STÖCKHERT, B. (1987): Das Uttenheimer Pegmatitfeld (Ostalpines Altkristallin, Südtirol) Genese und alpine Überprägung. - Erlanger geol. Abh., **114**: 83-106, Erlangen.

STÜWE, K. & POWELL, R. (1989): Low pressure granulite facies metamorphism in the Larsemann Hills area, East Antarctica; petrology and tectonic implications for the evolution of the Prydz Bay area. - J. metamorphic Geol., **7**: 465-483, Oxford.

THÖNI, M. (1981): Degree and evolution of the Alpine Metamorphism in the light of K/Ar and Rb/Sr age determinations on micas. - Jb. Geol. B.- A., **124/1**: 111-174, Wien.

THÖNI, M. (1983): The Climax of the Early Alpine Metamorphism in the Austroalpine Thrust Sheet. - Mem. Sci. Geol., **36**: 211–238, Padova.

THÖNI, M. (1999): A review of geochronological data from the Eastern Alps. - Schweiz. Mineral. Petrogr. Mitt., **79/1**: 209-230, Zürich.

THÖNI, M. & JAGOUTZ, E. (1992): Some new aspects of dating eclogites in orogenetic belts: Sm-Nd, Rb-Sr, and Pb-Pb isotopic results from the Austroalpine Saualpe and Koralpe type-locality (Carinthia/Styria, southern Austria). - Geochim. Cosmochim Acta, **56**: 347-368, Oxford.

THÖNI, M. & MILLER, CH. (2001): Permo-Triassic pegmatites in the eo-Alpine eclogite-facies Koralpe complex, Austria: age and magma source constraints from mineral chemical, Rb-Sr and Sm-Nd isotopic data. - Schweiz. Mineral. Petrogr. Mitt., **80**: 169-186, Zürich.

TOLLMANN, A. (1977): Geologie von Österreich. Band 1. Die Zentralalpen. - 1-766, (Deuticke) Wien.

TOLLMANN, A. (1985): Geologie von Österreich. Band 2. Außerzentralalpiner Anteil. - 1-710, (Deuticke) Wien.

TÖRÖK, K. (1999): Pre-Alpine development of the andalusite-sillimanite-biotite-schist from the Sopron Mountains (Eastern Alps, Western Hungary). - Acta Geol. Hung., **42/2**: 127-160,

Budapest.

TRIBUZIO, R., THIRLWALL, M.F. & MESSIGA, B. (1999): Petrology, mineral and isotope geochemistry of the Sondalo gabbroic complex (Central Alps, Northern Italy): implications for the origin of post-Variscan magmatism. - Contrib. Mineral. Petrol., **136**: 48-62, Heidelberg-New York.

TROPPER, P., BERNHARD, F. & KONZETT, J. (2001): Trace Element Mobility in Contact Metamorphic Rocks: Baddeleyite-Zirconolite-(Zircon) Veins in Olivine-Bearing Marbles from the Stubenberg Granite Contact Aureole (Styria, Austria). - EUG11, J. Conf. Abs. **6/1**: 278, Strasbourg.

TROPPER, P. & HOINKES, G., (1996): Geothermobarometry of Al2SiO5-bearing metapelites in the western Austroalpine Ötztal basement. Mineral. Petrol., **58:** 145-170, (Springer) Wien-New York.

VAI, G.B., COCOZZA, T. (1986): Tentative schematic zonation of the Hercynian chain in Italy. - Bull. Soc. Gèol France, **8/II**: 95-114, Paris.

VAVRA, G., GEBAUER, D., SCHMID, R. & COMPSTON, W. (1996): Multiple zircon growth and recrystallization during polyphase Late Carboniferous to Triassic metamorphism in granulites of the Ivrea Zone (Southern Alps): an ion microprobe (SHRIMP) study. - Contrib. Mineral. Petrol., **122**: 337-358, Heidelberg-New York.

WEISSENBACH, N. (1975): Gesteinsinhalt und Seriengliederung des Hochkristallins in der Saualpe. - Clausthaler geologische Abhandlungen, **Sbd. 1**: 61-114, Clausthal-Zellerfeld.

WERNIG, E. (1992): Tonale-, Pejo- and Judicarien-Linie: Kinematik, Mikrostrukturen und Metamorphose von Tektoniten aus räumlich interferierenden, aber verschiedenartigen Verwerfungszonen. - PhD thesis ETH Zürich, Zürich.

WOPFNER, H. (1984): Permian deposits of the Southern Alps as product of initial alpidic taphrogenesis. - Geol. Rundschau, **73**: 259-277, Stuttgart.

ZIEGLER, P.A. (1993): Late Palaeozoic-Early Mesozoic Plate Reorganisation: Evolution and Demise of the Variscan Fold Belt. - (In:) NEUBAUER, F. & VON RAUMER, J.F. (Eds.): The pre- Mesozoic Geology of the Alps: 203-216, Springer, Berlin-Heidelberg-New York.